



Published in final edited form as:

J Med Chem. 2013 January 10; 56(1): 15–30. doi:10.1021/jm301448p.

Discovery of potent myeloid cell leukemia 1 (Mcl 1) inhibitors using fragment based methods and structure based design

Anders Friberg, Dominico Vigil, Bin Zhao, R. Nathan Daniels, Jason P. Burke, Pedro M. Garcia-Barrantes, DeMarco Camper, Brian A. Chauder, Taekyu Lee, Edward T. Olejniczak, and Stephen W. Fesik*

Department of Biochemistry, Vanderbilt University School of Medicine, 2215 Garland Avenue, 607 Light Hall, Nashville, Tennessee 37232-0146, USA

Abstract

Myeloid cell leukemia-1 (Mcl-1), a member of the Bcl-2 family of proteins, is overexpressed and amplified in various cancers and promotes the aberrant survival of tumor cells that otherwise would undergo apoptosis. Here we describe the discovery of potent and selective Mcl-1 inhibitors using fragment-based methods and structure-based design. NMR-based screening of a large fragment library identified two chemically distinct hit series that bind to different sites on Mcl-1. Members of the two fragment classes were merged together to produce lead compounds that bind to Mcl-1 with a dissociation constant of <100 nM with selectivity for Mcl-1 over Bcl-xL and Bcl-2. Structures of merged compounds when complexed to Mcl-1 were obtained by X-ray crystallography and provide detailed information about the molecular recognition of small-molecule ligands binding Mcl-1. The compounds represent starting points for the discovery of clinically useful Mcl-1 inhibitors for the treatment of a wide variety of cancers.

Keywords

Fragment-based screening; apoptosis; cancer; Mcl-1; drug discovery

INTRODUCTION

Mcl-1 (Myeloid cell leukemia 1) is a member of the Bcl-2 family of proteins that when dysregulated prevents cancer cells from undergoing programmed cell death, a hallmark of cancer.¹ By overexpressing the Mcl-1 protein or amplifying the Mcl-1 gene, a cancerous cell can avoid death, the normal fate for cells exhibiting abnormal and deregulated growth.^{2,3} Indeed, amplification of Mcl-1 is one of the most common genetic aberrations observed in human cancer,^{4,5} including lung, breast, prostate, pancreatic, ovarian, and cervical cancers, as well as melanoma and leukemia.^{6–13} Moreover, Mcl-1 overexpression has emerged as a resistance mechanism against a number of anti-cancer therapies including the widely prescribed microtubule-targeted agents paclitaxel and vincristine¹⁴ as well as gemcitabine¹⁵, a first-line treatment option for pancreatic cancer. Mcl-1 overexpression also confers resistance to ABT-263, a Bcl-2/Bcl-xL inhibitor currently in clinical trials.^{16–18} Not

*Corresponding author stephen.fesik@vanderbilt.edu; Phone, +1 (615) 322 6303; Fax, +1 (615) 875 3236.

Supporting Information Mcl-1 protein sequence used for X-ray crystallography, 1H-15N HMQC spectra of Mcl-1 with and without compound 53, FPA dose-response curve of compound 53 displacing a FITC-labeled BAK peptide from Mcl-1 and synthesis of intermediates. This material is available free of charge via the Internet at <http://pubs.acs.org>.

ACCESSION CODES Atom coordinates and structure factors for Mcl-1/ligand complexes have been deposited at the Protein Data Bank (4HW2, 4HW3 and 4HW4).

surprisingly, specific down-regulation of Mcl-1 by RNA interference inhibits cell growth, colony formation, and induces apoptosis in pancreatic cancer cells *in vitro*, and markedly decreases tumorigenicity in mouse xenograft models.¹⁵ Silencing of Mcl-1 also potently kills particular subgroups of non-small-cell lung cancer (NSCLC) cell lines.¹⁹ Together, these data suggest that direct inhibition of Mcl-1 could be an effective therapeutic option for a wide variety of cancers. In an attempt to target Mcl-1 for the treatment of cancer, small-molecule inhibitors^{20–22} as well as stapled helix peptides^{23,24} that bind to Mcl-1 have been reported. However, no Mcl-1 inhibitors have entered clinical trials. Indeed, targeting Mcl-1 is extremely difficult, since Mcl-1 exerts its activity through protein-protein interactions involving a large binding interface. To overcome the challenges associated with targeting Mcl-1, we applied a combination of fragment-based methods²⁵ and structure-based design²⁶. A similar approach was successfully utilized in the discovery of ABT-263^{27,28} and in the discovery of inhibitors against other challenging protein targets, such as Hsp90²⁹ and BACE³⁰. Fragment-based drug discovery (FBDD) takes advantage of sensitive biophysical methods to detect the binding of molecular fragments (MW <300 Da) that bind weakly to their target proteins. This approach leads to a more efficient sampling of chemical space and can provide hits with higher ligand efficiencies.^{31,32} Furthermore, the affinity of the initial fragment hits can be markedly increased by growing, linking, or scaffold merging to obtain potent lead molecules.

Here, we describe the discovery of potent small-molecule Mcl-1 inhibitors ($K_i < 100$ nM) that inhibit BH3-containing peptides from binding to Mcl-1. An NMR-based fragment screen yielded two distinct classes of hits that were shown by NMR to bind to two different regions of Mcl-1. Based on NMR-derived structural information, the hits from the two classes were merged together to obtain potent Mcl-1 inhibitors that exhibited >100-fold enhanced binding affinity over each component separately. Improved analogs were rapidly optimized by exploiting the SAR observed for the initial fragment hits. Crystal structures of inhibitor-bound Mcl-1 complexes validate the design strategy and also provide detailed structural information for the discovery of more potent inhibitors.

RESULTS

Hit Identification

Recombinant, isotopically labeled Mcl-1 (residues 172–327) was used to screen our curated fragment library (>13,800 compounds) by recording SOFAST ¹H-¹⁵N HMQC spectra of Mcl-1 (Figure 1) incubated with mixtures of 12 fragments. Deconvolution of the mixtures by screening individual compounds yielded 132 hits (0.95% hit rate) of eleven distinct chemical classes. Of the initial hits, 93 inhibited Mcl-1 with a $K_i < 500$ μ M, and more than a quarter of the hits demonstrated a ligand efficiency (LE) of 0.25 or greater. Analogs were tested at a single concentration (400 μ M) for their ability to displace a FITC-labeled Mcl-1-derived BH3 peptide from binding to Mcl-1 in a fluorescence polarization anisotropy (FPA) assay.

Based on their affinity and distinct chemical characteristics, two classes of compounds were selected for follow-up experiments (Table 1). K_i values were derived from competition FPA assays measuring the disruption of Mcl-1 and a FITC-Mcl-1-BH3 peptide, or Bcl-xL and Bcl-2 and a FITC-BAK-BH3 peptide. Class I fragment hits contained 6,5-fused heterocyclic carboxylic acids. Analogs of the hits were obtained to explore the SAR. Parent benzothiophene-, benzofuran- and indole-2-carboxylic acids were not identified in our initial screen because of their weak affinity (**1**, **6** and **12**). The Class I fragment hits identified in the screen contained one or two Cl and/or Me substitutions which significantly improved their binding affinities. Similar trends in the SAR for all three core series suggest that they may display similar binding modes. The fragment SAR also suggests that the 3-, 4- and 6-

positions are preferred sites for substitutions, and that multiple substitutions can be tolerated or even beneficial in some combinations. For the indole series, a 1-Me substitution exerted similar effects as 3-Cl or 3-Me on benzothiophene and benzofuran scaffolds, suggesting that this core unit could be flipped along its long axis when bound. Interestingly, Mcl-1 inhibitors containing indole acids have also been recently reported in the patent literature.^{33,34}

Another structurally distinct group of fragment hits (Class II) consists of a hydrophobic aromatic system tethered by a linker to a polar functional group, most often a carboxylic acid (Table 1). Of the hits in this series, 4-chloro-3,5-dimethylphenyl and 1-naphthyl groups as contained in compounds **17** and **18**, respectively, were found to be preferred for binding to Mcl-1.

NOE-guided fragment docking

To determine how Class I and II fragments bind to Mcl-1, we performed NMR-based structural studies of Mcl-1/fragment hit complexes. Using double-labeled (¹⁵N, ¹³C) Mcl-1 protein, we acquired NOE-derived distance restraints and used these to dock representative fragments into a previously determined Mcl-1/Bim BH3 peptide complex (PDB: 3KJ2³⁵). Compounds were docked using a simulated annealing protocol in XplorNIH, followed by energy minimization of such models in MOE 2011.10 (Chemical Computing Group Inc.). Fragments representing Class I and II exhibited different patterns of protein/ligand NOEs confirming that they bind to different regions of Mcl-1. The model structures obtained by this method were consistent with the observed NOEs. A model for Mcl-1 complexed to a compound representative of Class I (compound **5**) is shown in Figure 2A. Compound **5** displayed NOEs from A227, M231, and F270 to the six-membered ring of the ligand. In this model the acid at the 2-position points towards R263. An NOE-derived model of a fragment hit representing Class II (compound **17**) is depicted in Figure 2B. In this case, NOEs from M250, F270, and V249 to the two methyl groups of the 4-chloro-3,5-dimethylphenyl indicate that this aromatic group sits deep in the pocket. Additional NOEs from V253 to the aliphatic tether show that the carboxylic acid sits at the surface of the pocket. The NMR-derived models demonstrate that the hydrophobic portions of the two classes of molecules bind to adjacent parts of a large pocket and that the carboxylic acids of both series point towards and likely interact with R263. These results explain the observation that Class I and Class II compounds are not able to bind simultaneously to Mcl-1.

Fragment merging and linker optimization

NOE-guided molecular modeling positioned the Class I heterocycles above the hydrophobic pocket utilized by the Class II compounds. This arrangement suggests that the attachment of Class II aromatic groups with a 2-4 atom linker to the 3-position of the Class I 6,5-fused heterocycles would lead to merged compounds that maintain the favorable hydrophobic contacts of both fragments to Mcl-1 as well as the interaction between the common carboxylic acid and R263 of Mcl-1. Support for this linking strategy was also obtained from compounds identified and tested from the Vanderbilt Institute of Chemical Biology chemical collection, compounds **19** and **20** (Table 1), that exhibited Mcl-1 binding affinities of 62 μ M and 87 μ M, respectively. In order to test this hypothesis, the fragment hits for which we obtained NMR-derived model structures (Figure 2) were linked together. Scaffold merging produced a compound with greater than two orders of magnitude improved binding affinity (Figure 3). To determine the optimum linker length, a 1-naphthyl group was connected to the benzothiophene- and benzofuran-2-carboxylic acid cores at the 3-position using two to four atom linkers. Table 2 summarizes the Mcl-1 binding affinities for merged compounds with varying linker lengths. The two series of compounds containing different core units showed a parallel SAR, and all merged compounds **21-26** exhibited markedly enhanced

binding affinity compared to the unsubstituted cores **1** and **6** confirming the validity of the linking strategy. Although the 2- and 3-atom linked compounds led to a significant increase in potency, the 4-atom linked compounds (e.g., **23** and **26**) yielded the most potent Mcl-1 inhibitors in the series, displaying sub-micromolar dissociation constants. Moreover, these compounds exhibited selectivity for binding to Mcl-1 over Bcl-xL and Bcl-2 (Table 2).

SAR of the merged compounds

To further improve the binding affinity to Mcl-1, the binding contribution of the hydrophobic group of the Class II fragments was investigated (Table 3). A library of indoles (**27-48**) tethered by the optimized 4-atom linker to various aromatic groups containing different substitution patterns and sizes was prepared. The parent indole **27** with an unsubstituted phenyl group ($K_i = 35 \mu\text{M}$) showed a marginal increase in affinity over the initial fragment hits in the class (**13-15**). Substitutions at the 2'-position (**28, 29**) on the phenyl group yielded only a minor increase in potency. However, potency was remarkably enhanced (20-fold) by mono-substitution of small groups at the 3'-position as demonstrated by compounds **30** and **31** containing 3'-Me and 3'-CF₃ substitutions, respectively. An increase in affinity was also observed for 4'-Cl substitutions as exemplified by compound **33**. When these beneficial groups were combined, the effect was additive. For example, compound **35** which contains a 3'-Me-4'-Cl-phenyl group displays a 90-fold improved potency over the parent molecule **27**. Indole **37** containing a 3',5'-diMe-4'-Cl-phenyl also exhibited a similar potency as **35**; whereas, increasing the size of the 3'-substitution resulted in a slight reduction in affinity as evidenced by compound **36**.

Bicyclic aromatic groups, such as 1'-naphthyl, 1'-(4'-Cl-naphthyl), and 1'-(5,6,7,8-tetrahydronaphthyl) as exemplified in compounds **42, 44, and 45**, exhibited comparable sub-micromolar binding affinities compared to compound **37**. Interestingly, compound **43** containing a 2'-naphthyl moiety was 20-fold less potent than its regioisomer **42**, indicating that the attachment position to this group is important for optimal binding to Mcl-1. The largest reduction in potency was observed for compounds **47** and **48** with nitrogen-containing heterocycles (6'-quinolinyl and 4'-indole) showing a 190- and 40-fold lower affinity compared to **42**. These observations indicate that binding in the lower part of the pocket is dictated by hydrophobic interactions and that polar moieties are not accommodated in the binding pocket of Mcl-1. Additional substitutions of the core indole nitrogen are also tolerated as shown in compounds **56-59**. This SAR trend strongly suggests that size, substitution pattern, and hydrophobicity of the aromatic group are all essential for binding to Mcl-1. Interestingly, most of the optimal groups identified from the data set were identical to the initial Class II fragment hits, demonstrating that the preliminary fragment SAR can guide the optimization of the linked compounds.

The initial fragment SAR indicated that substitutions at the 4- or 6-position are beneficial. The same principles were applied to further optimize the potency of the linked compounds. As expected from the SAR of the fragment hits, 6-Cl adducts (**52-55**) displayed a potency increase. In contrast, 4-Cl analogs (**49-51**) exhibited mixed results, suggesting that the anchoring unit might cause a subtle alteration in the binding conformation of the core unit. Merged compounds comprising benzothiophene and benzofuran scaffolds revealed similar SAR patterns as the indole series.

An additional linking strategy was explored by attaching compounds to the 1-position of the indole core (Table 4). Compounds **69-71** containing the optimized linker and anchor units retained comparable potency as the corresponding 3-substituted indoles. This demonstrates that the core indole can bind in a conformation flipped along its long axis as previously predicted from the SAR of the fragment hits. Finally, the importance of the 2-carboxylic

acid was evaluated by converting **71** to an amide as in compound **72**. This single modification resulted in a dramatic reduction in potency of at least 3-orders of magnitude. In line with previous results, merged compounds showed selectivity over Bcl-2 and Bcl-xL, respectively. Compound **53**, for example, is one of the most potent inhibitors of Mcl-1 ($K_i = 55$ nM, Supporting Information, Figure S1) and displays a 16-fold selectivity over Bcl-2 and 270-fold over Bcl-xL.

These results clearly demonstrate the effectiveness of fragment-based methods and a structure-guided fragment merging strategy as a very powerful approach for rapidly obtaining potent binders against target proteins. Additionally, the ability to translate the lessons learned from the SAR of the fragment hits to our merged compounds aided the optimization of our lead compounds.

X-ray structures of merged compounds complexed to Mcl-1

The three-dimensional structures of compounds representing different series of merged compounds in complex with Mcl-1 were obtained by X-ray crystallography (Table 5). As shown in Figure 4 for a representative member of both the benzothiophene and the indole series, the merged compounds occupy both pockets identified by NMR. The Mcl-1 inhibitors bind in the BH3 binding groove and explain why our compounds compete with BH3-peptides for binding to Mcl-1. The overall secondary structures of Mcl-1 in the Mcl-1/inhibitor complexes did not change upon binding the small molecules.^{23,36} However, ligand binding does result in several important structural changes near the binding pocket (Figure 5A,B). In compound-bound structures, a pronounced bend was observed in helix 4 ($\alpha 4$) which helps accommodate the anchor unit of the ligand in the deep hydrophobic pocket, and places the top of $\alpha 4$ closer to the ligand. In fact, the top of $\alpha 4$ protrudes slightly into the BH3 binding cleft. This causes the loop connecting helix 4-5 to be pulled towards the ligand and allows changes in the charge-charge interactions of R263 (Figure 5C,D). The guanidinium group of R263 can now interact with the carboxylate moiety of the merged compounds. These changes are not easily anticipated from the inspection of Mcl-1 complexed with a peptide. In peptide-bound structures, $\alpha 4$ is straight which keeps the BH3 binding cleft and the connecting loop open to better accommodate the peptide. The side chain of R263 also adopts a different conformation so that it can interact with D218 of the peptide (Figure 5C). It is also evident that the peptide does not utilize the full capacity of the hydrophobic pocket. In the peptide structure, L213 is only occupying the very upper part of this deep pocket (Figure 6A).

In all of the structures obtained thus far, the hydrophobic unit of the Class II fragments binds in the lower part of the pocket (Figure 4). Furthermore, all core units derived from Class I fragments are positioned in the upper part of the pocket, directing the carboxylic acid towards R263, and forming an interaction with M231, A227, F228, and F270 via the six-membered ring (Figure 4B).

The SAR of our merged compounds can now be rationalized from a more detailed analysis of the X-ray structures. Positions 1 and 7 of the core unit are surface exposed and, as shown, substitutions here have little or no effect on compound binding. In contrast, there is minimal space for any substitution at the 5-position which is consistent with results of the observed SAR. The results obtained when adding groups at the 4-position could be explained by slight differences in how the hydrophobic group and the linker are positioned. These subtle changes may affect how much room there is at the 4-position or how the entire core unit is positioned in the binding pocket. Insights regarding the improved affinity due to substitutions at the 6-position can be derived from the X-ray structures. The up to 5-fold increase in binding may be explained by the addition of a hydrophobic group, which fits between M231 and A227 in a previously unoccupied pocket (Figure 4B). Presumably the

chlorine keeps the core unit in a more favorable position so that the carboxylic acid can make a better interaction with R263 (Figure 5D). The latter interaction also explains the requirement of a negatively charged acidic group in our fragment hits as well as the loss of affinity upon amidation of the carboxylic acid (**71**, **72**).

The SAR of the Class II hits was also analyzed in terms of the X-ray structures. From the structures, it is evident why hydrophobic groups are preferred over more hydrophilic aromatic ring systems containing a nitrogen atom (compound **47** and **48**). The pocket is lined with numerous non-polar side chains, namely M231, L235, L246, V249, M250, L267, F270, V273, L290, and I294. An overlay of compounds **53** and **60** when bound to Mcl-1 show a precise overlap of the anchoring 3',5'-diMe-4-Cl-phenyl group (Figure 4A), suggesting that this unit anchors the rest of the ligand in the binding pocket. This binding pocket is present in both Bcl-xL and Bcl-2; however, it is neither as deep nor as large as it is in Mcl-1. Accessing parts of this pocket not present in other members of the Bcl-2 family provides a possible explanation for the selectivity of our compounds for binding to specific Bcl-2 family proteins.

SYNTHESIS

Compounds **21-26** and **60-68** were prepared as outlined in Scheme 1. Selective lithiation at the 3-Me position of compounds **80a-b** with LDA at $-10\text{ }^{\circ}\text{C}$ followed by nucleophilic substitution with 1-(bromoalkyl)naphthylenes or 1-(2-bromoethoxy)naphthalene gave compounds **21-26** with varying linker length to the terminal 1-naphthyl group. 3-Methylbenzothiophene-2-carboxylic acid cores **82a-c** containing 4-, 6- or 7-Cl substitutions were synthesized from the corresponding chloro-(2-fluorophenyl)ethanones (**81a-c**) by reacting with methyl thioglycolate under DBU followed by saponification of the produced esters. Compounds **82a-c** and **80a** were then subjected to the alkylation condition described above to yield compounds **60-66**. Unlike unsubstituted benzothiophene **80a**, it is necessary to employ alkyl iodides as substrates to increase yields due to reduced nucleophilicity of cores **82a-c** by the substituted chloride. 5-Cl-Benzofuran **84** was prepared from **83** by reacting with methyl bromoacetate. Using similar conditions, compounds **67** and **68** were obtained.

Mcl-1 inhibitors containing indole core **27-59** were synthesized by the route shown in Scheme 2. Indoles **85a-c** were prepared utilizing the modified Japp-Klingemann reaction.³⁷ Selective reduction using excess BH_3 gave the corresponding alcohols which were then treated with a variety of aromatic alcohols under Mitsunobu conditions to afford the corresponding ether **86**. The ester was then saponified to give indoles **27-55**. N-substituted indoles **56-59** were produced through alkylations of selected esters **86** followed by hydrolysis.

Class II fragments, binding in the deep hydrophobic pocket, can also be linked to the indole nitrogen as depicted in Scheme 3. Ethyl indole-2-carboxylate **88** was substituted at the 1-position with ethyl 3-bromopropionate using K_2CO_3 as a base under reflux in good yield. The adduct **89** then underwent the same series of reactions to give compounds **69-71**. Compound **71** was further functionalized by amidation to produce **72**.

DISCUSSION

Mcl-1 is one of the most frequently amplified genes in human cancers and a common resistance factor to treatment with current chemotherapeutic agents and existing Bcl-2 family inhibitors (e.g., ABT-263 and ABT-199).^{4,38} Here, we describe the discovery of small-molecules that potently inhibit Mcl-1 using fragment-based methods and structure-

based design. The X-ray structures of our merged compounds complexed with Mcl-1 identify several opportunities to significantly improve the affinity of the current lead molecules.

Although current lead compounds are able to compete with BH3-containing peptides for binding to Mcl-1, crystal structures reveal that the compounds may not be maximally exploiting the available binding opportunities. For example, pockets occupied by the peptide residues V216, D218, and V220 are currently not occupied by the compounds (Figure 6). Mutation of V216, D218, and V220 to alanine reduces peptide binding affinity 50-, 5-, and 45-fold, respectively, demonstrating the importance of these additional binding pockets.²³ Expanding our lead compounds to fill more of the peptide interface could yield more potent Mcl-1 inhibitors. In support of this hypothesis is a comparison of one of our current lead molecules bound to Mcl-1 with ABT-737 complexed to Bcl-xL (Figure 6B). Our lead compounds are much smaller than ABT-737, and only use a fraction of the binding pockets.

To identify small molecules that bind to these additional pockets, fragment-based screens of Mcl-1 in the presence of one of our nanomolar leads represents a possible strategy for improving potency. By blocking the initial site, fragments could be identified that bind to these additional pockets of the protein. These fragments could be rapidly incorporated into new molecules to markedly improve binding affinity.

An important lesson learned from these studies is that the SAR observed with the fragment hits is mirrored in the merged compounds and quickly led to the design and synthesis of potent lead molecules. In addition, the selectivity profile of the fragment hits for binding to Bcl-2 family members is mimicked by the merged compounds. The affinity of initial Mcl-1 fragment hits against the closely related family members Bcl-xL and Bcl-2 revealed a 5- to 50-fold selectivity for binding to Mcl-1 which is retained in the lead compounds.

In summary, this study demonstrates the successful targeting of Mcl-1 by fragment-based and structure-guided methods to quickly produce an initial set of high-affinity and Mcl-1 selective inhibitors. The compounds described here serve as starting points for the discovery of clinically useful Mcl-1 inhibitors for the treatment of cancer.

EXPERIMENTAL SECTION

Protein expression and purification

A codon-optimized gene sequence encoding residues 172-327 of human Mcl-1 (Uniprot: *Q07820*) was purchased (Genscript) and cloned into a Gateway entry vector (pDONR-221, Invitrogen) using the protocols provided (Supporting Information, Table S1). This construct was further sub-cloned into an expression vector (pDEST-HisMBP) containing a maltose binding protein (MBP) tag for increased solubility, a tobacco etch virus (TEV) protease recognition site for tag-removal and an N-terminal His-tag to facilitate purification. The integrity of all plasmids was checked by sequencing. Soluble Mcl-1 protein was expressed in *Escherichia coli* BL21 CodonPlus (DE3) RIL (Stratagene) using ampicillin and chloramphenicol for selection.

In brief, a colony from a fresh transformation plate was picked to inoculate 100 mL of LB medium (37°C). The overnight culture was used to start a 10 L fermentation (BioFlo 415, New Brunswick Scientific) grown at 37°C. For NMR studies, uniformly ¹⁵N and ¹⁵N/¹³C isotopically labeled protein samples were produced in minimal M9 media, where ¹⁵NH₄Cl and [U-¹³C]-D-glucose were used as sole nitrogen and carbon sources (Cambridge Isotope Laboratories). When the cell density corresponded to OD₆₀₀=2, the temperature was lowered to 20°C. After one hour, protein expression was induced with 0.5 mM IPTG. Cells

were harvested after 16 h by centrifugation. Pellets were frozen and re-dissolved in lysis buffer (20 mM TRIS pH 7.5, 300 mM NaCl, 20 mM imidazole, 5 mM BME), approximately 100 mL/10 g pellet, before the cells were broken by homogenization (APV-2000, APV). Prior to application to an affinity column (140 mL, ProBond, Invitrogen), lysate was cleared by centrifugation (18,000 rpm) and filtration (0.44 μ M). Bound protein was washed on the column and then eluted by a gradient (20 mM TRIS pH 7.5, 300 mM NaCl, 500 mM imidazole, 5 mM BME). To enhance TEV protease cleavage, samples were buffer exchanged (50 mM TRIS pH 7.5, 100 mM NaCl, 5 mM BME) on three serially connected columns (HiPrep 26/10 Desalting, GE Healthcare). TEV protease was added to a molar ratio of 1:10 (TEV:Mcl-1) and incubated at room temperature until cleavage was complete. After adding 20 mM imidazole to the samples, they were passed over a subtractive second nickel-column (120 mL, Ni-NTA Superflow, Qiagen) to remove the MBP-tag, non-cleaved protein, and TEV protease. Mcl-1 protein for NMR screening was buffer exchanged into an optimized NMR buffer (25 mM sodium phosphate pH 6.3, 25 mM NaCl, 1 mM DTT, 0.01% NaN_3). To achieve highly pure samples (e.g. for crystal screening), a supplementary step of size-exclusion chromatography (HiLoad 26/60, Superdex 75, GE Healthcare) was implemented. The running buffer also acted as the Mcl-1 storage and crystallography buffer (20 mM HEPES pH 6.8, 50 mM NaCl, 3 mM DTT, 0.01% NaN_3). Purifications were done at 4°C, and concentration steps were performed in stirred ultrafiltration cells (Amicon, Millipore).

To improve protein sample quality and to increase crystal diffraction, protein mutants were created by site-directed mutagenesis (QuikChange, Agilent Technologies). Primers for a C-terminal deletion ($\Delta 5$) were designed using their online tool and ordered from Eurofins MWG Operon. Mutations were made on the entry vector above, analyzed by in-house sequencing, and subsequently transferred into the pDEST-HisMBP expression vector. Mutant proteins were purified in the same way as wild-type (WT) proteins.

NMR experiments: Fragment screening and NOE-guided fragment docking

Nuclear magnetic resonance (NMR) screening experiments were performed at 30°C using either a Bruker Avance III 500-MHz or 600-MHz NMR spectrometer equipped with a 5-mm single-axis z-gradient cryo-probe and a Bruker Sample Jet sample changer. Two-dimensional, gradient-enhanced ^1H , ^{15}N heteronuclear multiple-quantum coherence (SOFAST-HMQC) spectra (32 scans, ~12 min) were used to track shift changes upon ligand binding.³⁹ Spectra were processed and analyzed in Topspin v3.1 (Bruker BioSpin). A fragment library comprising ~13,800 compounds which generally satisfy the “Rule of Three” (MW ≤ 300 , cLogP ≤ 3.0 , no more than 3 hydrogen bond donors)⁴⁰, and having no more than 4 rotatable bonds was screened as mixtures of 12 fragments. Samples (500 μ L) contained 50 μ M ^{15}N -labeled Mcl-1, 400 μ M of each fragment and 5% d_6 -DMSO. Deconvolution of hit mixtures was performed as single fragments. Recycling of the protein used for screening was accomplished by a simple buffer exchange with a yield of 50-80%.

NOE-derived distance restraints were acquired to enable NMR-based docking of fragments into a previously determined X-ray structure of a Mcl-1/peptide complex. Spectra were recorded on a Bruker 800-MHz spectrometer equipped with a cryo-probe and pulsed field gradients. 300 μ M $^{15}\text{N}/^{13}\text{C}$ -labeled samples of Mcl-1 was prepared in a D_2O -based NMR buffer and mixed with selected fragments at a concentration of 1 mM. Side-chain ^1H and ^{13}C NMR signals were assigned from ^{13}C -edited NOE and HCCH-TOCSY experiments.⁴¹ NOE distance restraints were obtained from three-dimensional ^{13}C -edited NOESY spectra, as well as three-dimensional ^{15}N - and ^{13}C -filter/edited NOESY spectra acquired with a mixing time of 80 ms. Compounds were docked into a X-ray structure of a Mcl-1/BIM peptide complex (PDB: 3KJ2) using the NMR-derived restraints and a simulated annealing protocol using the program Xplor-NIH.^{35,42} A square-well potential ($F_{\text{NOE}} = 50$

kcal mol⁻¹) was employed to constrain NOE-derived distances. Five low energy models from this process were energy minimized using MOE 2011.10 (Chemical Computing Group Inc., Montreal). The lowest energy structures obtained by this method were consistent with the observed NOEs.

Protein crystallization, data collection and structure refinement

Fresh batches of Mcl-1 proteins, WT and Δ5, were concentrated to 600 μM (10.7 mg/mL) and 1 mM (17.4 mg/mL), respectively, and screened for crystallization conditions with a 1.2x excess of ligand. Crystals were obtained by mixing 1 μL protein with 1 μL reservoir solution (25-30% PEG 3350, 0.1 M Bis-TRIS pH 6.5, 0.2 M MgCl₂) as a hanging drop at 4°C or 18°C. Crystals appeared within the first week and were flash frozen in liquid nitrogen after cryoprotection using 10-20% glycol.

Data were collected on the Life Sciences Collaborative Access Team (LS-CAT) 21-ID-D beamline at the Advanced Photon Source (APS), Argonne National Laboratory. Indexing, integration and scaling was performed with HKL2000.⁴³ Using a previously determined peptide-bound structure (PDB: 3MK8), phasing was done by molecular replacement with Phaser⁴⁴ as implemented in CCP4⁴⁵. Refinement of the structural models were performed with Phenix⁴⁶ and Refmac⁴⁷, and included rounds of manual model building in COOT⁴⁸. Figures were prepared in PyMOL⁴⁹ and MOE.

FPA Competition Assays

Fluorescein isothiocyanate (FITC)-labeled Mcl-1-BH3 peptide (FITC-AHx-KALETLRRVGDGVQRNHETAFAF-NH2)²³ and FITC-Bak-BH3 peptide (FITC-AHx-GQVGRQLAIIGDDINR-NH2) were purchased from GenScript and used without further purification. FPA measurements were carried out in 384-well, black, flat-bottom plates (Greiner Bio-One) using the EnVision plate reader (PerkinElmer). All assays were conducted in assay buffer containing 20 mM TRIS pH 7.5, 50 mM NaCl, 3 mM DTT, and 2% DMSO. To measure inhibition of the Mcl-1/FITC-Mcl-1-BH3 interaction, Mcl-1 and FITC-Mcl-1-BH3 peptide were each added at 250 nM. To measure inhibition of the FITC-Bak-BH3 interaction with Bcl-2 family members, 10nM FITC-Bak-BH3 peptide was incubated with either 14 nM Mcl-1, 4 nM Bcl-xL, or 40 nM Bcl-2. For IC₅₀ determination, compounds were diluted in DMSO in a 16-point, 2-fold serial dilution scheme, added to assay plates, and incubated for 1 hour at room temperature. The change in anisotropy was measured and used to calculate an IC₅₀ (inhibitor concentration at which 50% of bound peptide is displaced), by fitting the inhibition data using XLFit software (Guildford, UK), to a single-site binding model. This was converted into a binding dissociation constant (K_i) according to the formula⁵⁰:

$$K_i = [I]_{50} / \left([L]_{50} / K_d^{\text{pep}} + [P]_0 / K_d^{\text{pep}} + 1 \right)$$

where [I]₅₀ is the concentration of the free inhibitor at 50% inhibition, [L]₅₀ is the concentration of the free labeled ligand at 50% inhibition, [P]₀ is the concentration of the free protein at 0% inhibition and K_d^{pep} represents the dissociation constant of the FITC-labeled peptide probe.

CHEMISTRY

General

All NMR spectra were recorded at room temperature on a 400 MHz AMX Bruker spectrometer. ¹H chemical shifts are reported in δ values in ppm downfield with the

deuterated solvent as the internal standard. Data are reported as follows: chemical shift, multiplicity (s = singlet, d = doublet, t = triplet, q = quartet, br = broad, m = multiplet), integration, coupling constant (Hz). Low resolution mass spectra were obtained on an Agilent 1200 series 6140 mass spectrometer with electrospray ionization. All samples were of >95% purity as analyzed by LC-UV/vis-MS. Analytical HPLC was performed on an Agilent 1200 series with UV detection at 214 and 254 nm along with ELSD detection. LC/MS parameters were as follows: Phenomenex-C18 Kinetex column, 50 × 2.1 mm, 2 min gradient, 5% (0.1% TFA/MeCN) / 95% (0.1% TFA/H₂O) to 100% (0.1% TFA/MeCN). Preparative purification was performed on a Gilson HPLC (Phenomenex-C18, 100 × 30 mm, 10 min gradient, 5→95% MeCN/H₂O with 0.1% TFA) or by automated flash column chromatography (Isco, Inc. 100sg Combiflash). Solvents for extraction, washing, and chromatography were HPLC grade. All reagents were purchased from chemical suppliers and used without purification.

3-(2-(naphthalen-1-yl)ethyl)benzo[b]thiophene-2-carboxylic acid (21): General procedure for alkylation of 3-methylbenzothiophene or 3-methylbenzofuran-2-carboxylic acid

To a stirred solution of 3-methylbenzo[b]thiophene-2-carboxylic acid (101 mg, 0.53 mmol) in anhydrous THF (5.0 mL) was added LDA (0.58 mL, 1.17 mmol, 2 M in THF) dropwise under Ar at -10 °C. The reaction mixture was stirred for 30 min then a solution of 1-(bromomethyl)naphthalene (116 mg, 0.525 mmol) in THF (2 mL) was added dropwise. The reaction mixture was stirred for an additional 1 h at -10 °C then warm to room temperature and stirred overnight. The reaction was quenched by addition of saturated NH₄Cl aq. solution and extracted with CH₂Cl₂ (2 × 20 mL). The organic extracts were combined, concentrated and the residue was purified by reverse phase prep HPLC to give the product as a solid (103 mg, 0.310 mmol). ¹H NMR (400 MHz, d₆-DMSO): δ (ppm) 8.37 (d, *J* = 8.2 Hz, 1H), 8.02 (d, *J* = 8.0 Hz, 1H), 7.93 (d, *J* = 8.0 Hz, 2H), 7.79 (dd, *J* = 7.2, 1.8 Hz, 1H), 7.53 (m, 3H), 7.44 (m, 3H), 3.61 (m, 2H), 3.33 (m, 2H); >98% @215 nm, MS (ESI) *m/z* = 333.3 (M+H)⁺.

3-(3-(naphthalen-1-yl)propyl)benzo[b]thiophene-2-carboxylic acid (22)

The general procedure for alkylation was followed using 3-methylbenzo[b]thiophene-2-carboxylic acid (86 mg, 0.45 mmol) and 1-(2-bromoethyl)naphthalene (105 mg, 0.45 mmol) to yield the title compound (78 mg, 0.23 mmol). ¹H NMR (400 MHz, d₆-DMSO): δ (ppm) 7.96 (m, 2H), 7.88 (m, 2H), 7.75 (d, *J* = 7.5 Hz, 1H), 7.48 (m, 3H), 7.40 (m, 3H), 3.41 (t, *J* = 7.7 Hz, 2H), 3.15 (t, *J* = 7.8 Hz, 2H), 1.99 (p, *J* = 7.7 Hz, 2H); >98% @215 nm, MS (ESI) *m/z* = 369.1 (M+Na)⁺.

3-(3-(naphthalen-1-yloxy)propyl)benzo[b]thiophene-2-carboxylic acid (23)

The general procedure for alkylation was followed using 3-methylbenzo[b]thiophene-2-carboxylic acid (100 mg, 0.52 mmol) and 1-(2-bromoethoxy)naphthalene (131 mg, 0.52 mmol) to yield the title compound (101 mg, 0.28 mmol). ¹H NMR (400 MHz, d₆-DMSO): δ (ppm) 8.18 (d, *J* = 7.8 Hz, 1H), 8.01 (t, *J* = 7.9 Hz, 2H), 7.85 (m, 1H), 7.48 (m, 4H), 7.37 (m, 2H), 6.89 (d, *J* = 7.4 Hz, 1H), 4.21 (t, *J* = 5.9, 2H), 3.54 (t, *J* = 7.6, 2H), 2.20 (m, 2H); >98% @215 nm, MS (ESI) *m/z* = 363.1 (M+H)⁺.

3-(3-(4-chloro-3,5-dimethylphenoxy)propyl)benzo[b]thiophene-2-carboxylic acid (60)

The general procedure for alkylation was followed using 3-methylbenzo[b]thiophene-2-carboxylic acid (97 mg, 0.50 mmol) and 5-(2-bromoethoxy)-2-chloro-1,3-dimethylbenzene (133 mg, 0.50 mmol) to yield the title compound (89 mg, 0.24 mmol). ¹H NMR (400 MHz, d₆-DMSO): δ (ppm) 8.00 (d, *J* = 8.1 Hz, 1H), 7.96 (d, *J* = 8.1 Hz, 1H), 7.50 (t, *J* = 7.5 Hz,

1H), 7.42 (t, $J = 7.6$ Hz, 1H), 6.74 (s, 2H), 3.98 (t, $J = 6.2$ Hz, 2H), 3.38 (t, $J = 7.5$, 2H), 2.26 (s, 6H), 2.01 (p, $J = 7.2$, 2H); >98% @215 nm, MS (ESI) $m/z = 375.1$ (M+H)⁺.

4-chloro-3-(3-(4-chloro-3,5-dimethylphenoxy)propyl)benzo[b]thiophene-2-carboxylic acid (61)

The general procedure for alkylation was followed using 4-chloro-3-methylbenzo[b]thiophene-2-carboxylic acid (57 mg, 0.25 mmol) and 2-chloro-5-(2-iodoethoxy)-1,3-dimethylbenzene (78 mg, 0.25 mmol) to yield the title compound (25.6 mg, 0.063 mmol). ¹H NMR (400 MHz, d₆-DMSO): δ (ppm) 8.01 (dd, $J = 7.7$, 1.1 Hz, 1H), 7.49 (m, 2H), 6.73 (s, 2H), 4.05 (t, $J = 6.2$ Hz, 2H), 3.70 (m, 2H), 2.26 (s, 6H), 2.05 (m, 2H); >98% @215 nm, MS (ESI) $m/z = 409.1$ (M+H)⁺.

4-chloro-3-(3-(naphthalen-1-yloxy)propyl)benzo[b]thiophene-2-carboxylic acid (62)

The general procedure for alkylation was followed using 4-chloro-3-methylbenzo[b]thiophene-2-carboxylic acid (57 mg, 0.25 mmol) and 1-(2-iodoethoxy)naphthalene (75 mg, 0.25 mmol) to yield the title compound (9.9 mg, 0.025 mmol). ¹H NMR (400 MHz, d₆-DMSO): δ (ppm) 8.15 (d, $J = 8.0$ Hz, 1H), 8.02 (m, 1H), 7.85 (d, $J = 7.9$ Hz, 1H), 7.46 (m, 6H), 6.96 (d, $J = 7.2$ Hz, 1H), 4.28 (t, $J = 5.9$, 2H), 3.87 (m, 2H), 2.23 (m, 2H); >98% @215 nm, MS (ESI) $m/z = 419.1$ (M+Na)⁺.

6-chloro-3-(3-(4-chloro-3,5-dimethylphenoxy)propyl)benzo[b]thiophene-2-carboxylic acid (63)

The general procedure for alkylation was followed using 6-chloro-3-methylbenzo[b]thiophene-2-carboxylic acid (57 mg, 0.25 mmol) and 2-chloro-5-(2-iodoethoxy)-1,3-dimethylbenzene (78 mg, 0.25 mmol) to yield the title compound (36 mg, 0.087 mmol). ¹H NMR (400 MHz, d₆-DMSO): δ (ppm) 8.18 (d, $J = 1.9$ Hz, 1H), 7.97 (d, $J = 8.7$ Hz, 1H), 7.45 (dd, $J = 8.7$, 1.9 Hz, 1H), 6.70 (s, 2H), 3.96 (t, $J = 6.2$ Hz, 2H), 3.36 (m, 2H), 2.26 (s, 6H), 2.00 (p, $J = 7.2$ Hz, 2H); >98% @215 nm, MS (ESI) $m/z = 431.1$ (M+Na)⁺.

6-chloro-3-(3-(naphthalen-1-yloxy)propyl)benzo[b]thiophene-2-carboxylic acid (64)

The general procedure for alkylation was followed using 6-chloro-3-methylbenzo[b]thiophene-2-carboxylic acid (57 mg, 0.25 mmol) and 1-(2-iodoethoxy)naphthalene (75 mg, 0.25 mmol) to yield the title compound (9.9 mg, 0.025 mmol). ¹H NMR (400 MHz, d₆-DMSO): δ (ppm) 8.17 (d, $J = 1.9$ Hz, 1H), 8.12 (d, $J = 8.0$ Hz, 1H), 8.02 (d, $J = 8.8$ Hz, 1H), 7.84 (d, $J = 7.7$ Hz, 1H), 7.48 (m, 3H), 7.38 (m, 2H), 6.89 (d, $J = 7.4$ Hz, 1H), 4.20 (t, $J = 5.9$, 2H), 3.52 (t, $J = 7.6$, 2H), 2.18 (m, 2H); >98% @215 nm, MS (ESI) $m/z = 419.1$ (M+Na)⁺.

7-chloro-3-(3-(4-chloro-3,5-dimethylphenoxy)propyl)benzo[b]thiophene-2-carboxylic acid (65)

The general procedure for alkylation was followed using 7-chloro-3-methylbenzo[b]thiophene-2-carboxylic acid (57 mg, 0.25 mmol) and 2-chloro-5-(2-iodoethoxy)-1,3-dimethylbenzene (78 mg, 0.25 mmol) to yield the title compound (53 mg, 0.13 mmol). ¹H NMR (400 MHz, d₆-DMSO): δ (ppm) 7.97 (d, $J = 8.1$ Hz, 1H), 7.64 (d, $J = 7.6$ Hz, 1H), 7.47 (t, $J = 7.9$ Hz, 1H), 6.70 (s, 2H), 3.97 (t, $J = 6.1$ Hz, 2H), 3.38 (m, 2H), 2.25 (s, 6H), 2.02 (p, $J = 7.1$ Hz, 2H); MS (ESI) $m/z = 409.1$ (M+H)⁺.

7-chloro-3-(3-(naphthalen-1-yloxy)propyl)benzo[b]thiophene-2-carboxylic acid (66)

The general procedure for alkylation was followed using 7-chloro-3-methylbenzo[b]thiophene-2-carboxylic acid (57 mg, 0.25 mmol) and 1-(2-

iodoethoxy)naphthalene (75 mg, 0.25 mmol) to yield the title compound (25 mg, 0.062 mmol) $^1\text{H NMR}$ (400 MHz, d_6 -DMSO): δ (ppm) 8.05 (d, $J = 8.2$ Hz, 1H), 8.02 (d, $J = 8.1$ Hz, 1H), 7.84 (d, $J = 8.0$ Hz, 1H), 7.61 (d, $J = 7.6$ Hz, 1H), 7.50 (m, 1H), 7.41 (m, 4H), 6.88 (d, $J = 7.5$ Hz, 1H), 4.20 (t, $J = 5.8$, 2H), 3.54 (t, $J = 7.5$, 2H), 2.21 (p, $J = 7.1$ Hz, 2H); MS (ESI) $m/z = 397.0$ (M+H) $^+$.

3-(3-(naphthalen-1-yl)propyl)benzofuran-2-carboxylic acid (24)

The general procedure for alkylation was followed using 3-methylbenzofuran-2-carboxylic acid and 1-(bromomethyl)naphthalene to yield the title compound. $^1\text{H NMR}$ (400 MHz, CDCl_3) δ (ppm) 8.26 (d, 1H, $J = 8.4$ Hz), 7.91 (d, 1H, $J = 8.4$ Hz), 7.75 (d, 1H, $J = 8.2$ Hz), 7.32-7.62 (m, 8H), 3.48-3.59 (m, 4H); >98% @215 nm, MS (ESI) $m/z = 317.0$ (M+H) $^+$.

3-(2-(naphthalen-1-yl)ethyl)benzofuran-2-carboxylic acid (25)

The general procedure for alkylation was followed using 3-methylbenzofuran-2-carboxylic acid and 1-(2-bromoethyl)naphthalene to yield the title compound. $^1\text{H NMR}$ (400 MHz, CDCl_3) δ (ppm) 8.26 (d, 1H, $J = 8.6$ Hz), 7.32-7.97 (m, 10H), 3.42-3.59 (m, 2H), 3.17-3.36 (m, 2H), 2.18-2.30 (m, 2H); >98% @215 nm, MS (ESI) $m/z = 331.0$ (M+H) $^+$.

3-(3-(naphthalen-1-yloxy)propyl)benzofuran-2-carboxylic acid (26)

The general procedure for alkylation was followed using 3-methylbenzofuran-2-carboxylic acid and 1-(2-bromoethoxy)naphthalene to yield the title compound. $^1\text{H NMR}$ (400 MHz, CDCl_3) δ (ppm) 8.26 (d, 1H, $J = 8.6$ Hz), 7.32-7.97 (m, 10H), 4.01 (m, 2H), 3.32 (m, 2H), 2.28 (m, 2H); >98% @215 nm, MS (ESI) $m/z = 347.2$ (M+H) $^+$.

3-(3-(4-chloro-3,5-dimethylphenoxy)propyl)benzofuran-2-carboxylic acid (67)

The general procedure for alkylation was followed using 3-methylbenzofuran-2-carboxylic acid and 2-chloro-5-(2-bromoethoxy)-1,3-dimethylbenzene to yield the title compound. $^1\text{H NMR}$ (400 MHz, CDCl_3) δ (ppm) 7.71 (d, $J = 8.4$ Hz, 1H), 7.59 (d, $J = 8.6$ Hz, 1H), 7.49-7.54 (m, 1H), 7.28-7.34 (m, 1H), 6.62 (s, 2H), 3.99 (t, $J = 6.0$ Hz, 2H), 3.32 (t, $J = 7.4$ Hz, 2H), 2.34 (s, 6H), 2.23 (m, 2H); >98% @215 nm, MS (ESI) $m/z = 359.1$ (M+H) $^+$.

5-chloro-3-(3-(naphthalen-1-yloxy)propyl)benzofuran-2-carboxylic acid (68)

The general procedure for alkylation was followed using 5-chloro-3-methylbenzofuran-2-carboxylic acid⁵¹ and 1-(2-bromoethoxy)naphthalene to yield the title compound. >98% @215 nm, MS (ESI) $m/z = 381.1$ (M+H) $^+$.

3-(3-phenoxypropyl)-1H-indole-2-carboxylic acid (27): General procedure for phenol analogue coupling and saponification

To a solution of ethyl 3-(3-hydroxypropyl)-1H-indole-2-carboxylate (70 mg, 0.28 mmol), PPh_3 (110 mg, 0.51 mmol) and phenol (49 mg, 0.52 mmol) in THF (3.5 mL) was added Dt-BuAD (99 mg, 0.51 mmol) at 20 °C. The reaction mixture was stirred for 15h at 20 °C then concentrated *in vacuo*. The residue was purified by flash chromatography (Combi-flash Rf Hexane/EtOAc gradient 0-10%) to give ethyl 3-(3-phenoxypropyl)-1H-indole-2-carboxylic acid the title compound (92 mg, 0.25 mmol) as a colorless oil. >98% @215 nm, MS (ESI) $m/z = 324.1$ (M+H) $^+$.

To a solution of the ethyl ester (28 mg, 0.085 mmol) in EtOH (1.0 mL) was added 50% NaOH H_2O solution (50 μL) at 20 °C. The reaction mixture was stirred for 15h at 20 °C. The reaction mixture was acidified with 1N HCl solution, extracted with EtOAc, dried over MgSO_4 , filtered and concentrated *in vacuo*. The crude product was purified by reverse phase prep. HPLC ($\text{H}_2\text{O}/\text{CH}_3\text{CN}$ gradient to 95% CH_3CN 0.5% TFA) to yield the title compound

(23 mg, 0.078 mmol) as a white solid. ^1H NMR (400MHz, d_6 -DMSO): δ (ppm) 11.43 (s, 1H), 7.64. (d, J = 8.0 Hz, 1H), 7.39 (d, J = 8.4 Hz, 1H), 7.20 – 7.31 (m, 3H), 7.00 (t, J = 7.2 Hz, 1H), 6.89 – 6.99 (m, 3H), 3.95 (t, J = 6.4 Hz, 2H), 3.21 (t, J = 6.4 Hz, 2H), 2.01 - 2.10 (m, 2H); >98% @215 nm, MS (ESI) m/z = 296.1 [M+H] $^+$.

Compounds **28** - **55** were prepared following the general procedure outlined above in library format. Purity of all final compounds was determined by HPLC analysis is >95%. All compounds were isolated as solids.

3-(3-(*o*-tolylloxy)propyl)-1*H*-indole-2-carboxylic acid (28)

Coupling of ethyl 3-(3-hydroxypropyl)-1*H*-indole-2-carboxylate and *o*-cresol yielded **28**. ^1H NMR (400MHz, d_6 -DMSO): δ (ppm) 11.39 (s, 1H), 7.64. (d, J = 8.0 Hz, 1H), 7.40 (d, J = 8.4 Hz, 1H), 7.22 (t, J = 7.2 Hz, 1H), 7.13 (t, J = 8.0 Hz, 1H), 7.02 (t, J = 7.2 Hz, 1H), 6.67 – 6.76 (m, 3H), 3.94 (t, J = 6.4 Hz, 2H), 3.20 (t, J = 6.4 Hz, 2H), 2.25 (s, 3H), 2.01 - 2.11 (m, 2H); >98% @215 nm, MS (ESI) m/z = 310.1 [M+H] $^+$.

3-(3-(2-(trifluoromethyl)phenoxy)propyl)-1*H*-indole-2-carboxylic acid (29)

Coupling of ethyl 3-(3-hydroxypropyl)-1*H*-indole-2-carboxylate and 2-(trifluoromethyl)phenol yielded **29**. ^1H NMR (400MHz, d_6 -DMSO): δ (ppm) 11.43 (s, 1H), 7.64. (d, J = 8.0 Hz, 1H), 7.50 (t, J = 7.2 Hz, 1H), 7.39 (d, J = 8.4 Hz, 1H), 7.16 – 7.35 (m, 4H), 6.98 (t, J = 7.2 Hz, 1H), 4.04 (t, J = 6.4 Hz, 2H), 3.22 (t, J = 6.4 Hz, 2H), 2.01 - 2.12 (m, 2H); >98% @215 nm, MS (ESI) m/z = 364.1 [M+H] $^+$.

3-(3-(*m*-tolylloxy)propyl)-1*H*-indole-2-carboxylic acid (30)

Coupling of ethyl 3-(3-hydroxypropyl)-1*H*-indole-2-carboxylate and *m*-cresol yielded **30**. ^1H NMR (400MHz, d_6 -DMSO): δ (ppm) 11.39 (s, 1H), 7.64. (d, J = 8.0 Hz, 1H), 7.40 (d, J = 8.4 Hz, 1H), 7.22 (t, J = 7.2 Hz, 1H), 7.13 (t, J = 8.0 Hz, 1H), 7.02 (t, J = 7.2 Hz, 1H), 6.67 – 6.76 (m, 3H), 3.94 (t, J = 6.4 Hz, 2H), 3.20 (t, J = 6.4 Hz, 2H), 2.25 (s, 3H), 2.01 - 2.11 (m, 2H); >98% @215 nm, MS (ESI) m/z = 310.1 [M+H] $^+$.

3-(3-(3-(trifluoromethyl)phenoxy)propyl)-1*H*-indole-2-carboxylic acid (31)

Coupling of ethyl 3-(3-hydroxypropyl)-1*H*-indole-2-carboxylate and 3-(trifluoromethyl)phenol yielded **31**. ^1H NMR (400MHz, d_6 -DMSO): δ (ppm) 11.43 (s, 1H), 7.64. (d, J = 8.0 Hz, 1H), 7.50 (t, J = 7.2 Hz, 1H), 7.39 (d, J = 8.4 Hz, 1H), 7.16 – 7.35 (m, 4H), 6.98 (t, J = 7.2 Hz, 1H), 4.04 (t, J = 6.4 Hz, 2H), 3.22 (t, J = 6.4 Hz, 2H), 2.01 - 2.12 (m, 2H); >98% @215 nm, MS (ESI) m/z = 364.1 [M+H] $^+$.

3-(3-(*p*-tolylloxy)propyl)-1*H*-indole-2-carboxylic acid (32)

Coupling of ethyl 3-(3-hydroxypropyl)-1*H*-indole-2-carboxylate and *p*-cresol yielded **32**. ^1H NMR (400MHz, d_6 -DMSO): δ (ppm) 11.41 (s, 1H), 7.63 (d, J = 8.0 Hz, 1H), 7.39 (d, J = 8.0 Hz, 1H), 7.22 (t, J = 7.2 Hz, 1H), 7.06 (d, J = 8.0 Hz, 2H), 7.02 (t, J = 7.2 Hz, 1H), 6.79 (d, J = 8.4 Hz, 2H), 3.91 (t, J = 6.4 Hz, 2H), 3.19 (t, J = 6.4 Hz, 2H), 2.22 (s, 3H), 1.98 - 2.09 (m, 2H); >98% @215 nm, MS (ESI) m/z = 310.1 [M+H] $^+$.

3-(3-(4-chlorophenoxy)propyl)-1*H*-indole-2-carboxylic acid (33)

Coupling of ethyl 3-(3-hydroxypropyl)-1*H*-indole-2-carboxylate and 4-chlorophenol yielded **33**. ^1H NMR (400MHz, d_6 -DMSO): δ (ppm) 11.42 (s, 1H), 7.63 (d, J = 8.0 Hz, 1H), 7.39 (d, J = 8.4 Hz, 1H), 7.30 (d, J = 8.8 Hz, 2H), 7.22 (t, J = 7.2 Hz, 1H), 6.99 (t, J = 7.2 Hz, 1H), 6.93 (d, J = 8.8 Hz, 2H), 3.94 (t, J = 6.4 Hz, 2H), 3.19 (t, J = 6.4 Hz, 2H), 2.00 - 2.10 (m, 2H); >98% @215 nm, MS (ESI) m/z = 330.1 [M+H] $^+$.

3-(3-(4-(trifluoromethyl)phenoxy)propyl)-1H-indole-2-carboxylic acid (34)

Coupling of ethyl 3-(3-hydroxypropyl)-1*H*-indole-2-carboxylate and 4-(trifluoromethyl)phenol yielded **34**. ¹H NMR (400MHz, d₆-DMSO): δ (ppm) 11.43 (s, 1H), 7.60 – 7.69 (m, 3H), 7.39 (d, *J* = 8.4 Hz, 1H), 7.22 (t, *J* = 7.2 Hz, 1H), 7.08 (d, *J* = 8.4 Hz, 2H), 6.99 (t, *J* = 7.2 Hz, 1H), 4.04 (t, *J* = 6.4 Hz, 2H), 3.22 (t, *J* = 6.4 Hz, 2H), 2.03 - 2.13 (m, 2H); >98% @215 nm, MS (ESI) *m/z* = 364.1 [M+H]⁺.

3-(3-(4-chloro-3-methylphenoxy)propyl)-1H-indole-2-carboxylic acid (35)

Coupling of ethyl 3-(3-hydroxypropyl)-1*H*-indole-2-carboxylate and 4-chloro-3-methylphenol yielded **35**. ¹H NMR (400MHz, d₆-DMSO): δ (ppm) 11.42 (s, 1H), 7.63 (d, *J* = 8.0 Hz, 1H), 7.39 (d, *J* = 8.4 Hz, 1H), 7.18 – 7.30 (m, 2H), 7.00 (t, *J* = 7.6 Hz, 1H), 6.85 (s, 1H), 6.75 (d, *J* = 8.4 Hz, 1H), 3.94 (t, *J* = 6.4 Hz, 2H), 3.19 (t, *J* = 6.8 Hz, 2H), 2.24 (s, 3H), 1.95 - 2.10 (m, 2H); >98% @215 nm, MS (ESI) *m/z* = 344.1 [M+H]⁺.

3-(3-(4-chloro-3-ethylphenoxy)propyl)-1H-indole-2-carboxylic acid (36)

Coupling of ethyl 3-(3-hydroxypropyl)-1*H*-indole-2-carboxylate and 4-chloro-3-ethylphenol yielded **36**. ¹H NMR (400MHz, d₆-DMSO): δ (ppm) 11.42 (s, 1H), 7.63 (d, *J* = 8.0 Hz, 1H), 7.39 (d, *J* = 8.4 Hz, 1H), 7.26 (d, *J* = 8.8 Hz, 1H), 7.22 (t, *J* = 8.0 Hz, 1H), 7.02 (t, *J* = 8.0 Hz, 1H), 6.87 (s, 1H), 6.76 (d, *J* = 8.8 Hz, 1H), 3.95 (t, *J* = 6.4 Hz, 2H), 3.20 (t, *J* = 6.8 Hz, 2H), 2.61 (q, *J* = 7.6 Hz, 2H), 1.95 - 2.10 (m, 2H), 1.15 (t, *J* = 7.6 Hz, 3H); >98% @215 nm, MS (ESI) *m/z* = 358.1 [M+H]⁺.

3-(3-(4-chloro-3,5-dimethylphenoxy)propyl)-1H-indole-2-carboxylic acid (37)

Coupling of ethyl 3-(3-hydroxypropyl)-1*H*-indole-2-carboxylate and 4-chloro-3,5-dimethylphenol yielded **37**. ¹H NMR (400MHz, d₆-DMSO): δ (ppm) 11.42 (s, 1H), 7.63 (d, *J* = 8.0 Hz, 1H), 7.39 (d, *J* = 8.4 Hz, 1H), 7.22 (t, *J* = 7.6 Hz, 1H), 7.00 (t, *J* = 7.6 Hz, 1H), 6.74 (s, 2H), 3.93 (t, *J* = 6.4 Hz, 2H), 3.19 (t, *J* = 6.8 Hz, 2H), 2.27 (s, 6H), 1.95 - 2.10 (m, 2H); >98% @215 nm, MS (ESI) *m/z* = 358.1 [M+H]⁺.

3-(3-([1,1'-biphenyl]-3-yloxy)propyl)-1H-indole-2-carboxylic acid (38)

Coupling of ethyl 3-(3-hydroxypropyl)-1*H*-indole-2-carboxylate and [1,1'-biphenyl]-3-ol yielded **38**. ¹H NMR (400MHz, d₆-DMSO): δ (ppm) 11.43 (s, 1H), 7.55 - 7.75 (m, 3H), 7.31 – 7.52 (m, 5H), 7.25 – 7.46 (m, 3H), 6.98 - 7.03 (m, 1H), 6.91 (d, *J* = 8.0 Hz, 1H), 4.05 (t, *J* = 6.4 Hz, 2H), 3.23 (t, *J* = 6.4 Hz, 2H), 2.01 - 2.10 (m, 2H); >98% @215 nm, MS (ESI) *m/z* = 372.1 [M+H]⁺.

3-(3-([1,1'-biphenyl]-4-yloxy)propyl)-1H-indole-2-carboxylic acid (39)

Coupling of ethyl 3-(3-hydroxypropyl)-1*H*-indole-2-carboxylate and [1,1'-biphenyl]-4-ol yielded **39**. ¹H NMR (400MHz, d₆-DMSO): δ (ppm) 11.42 (s, 1H), 7.66 (d, *J* = 8.0 Hz, 1H), 7.63 – 7.52 (m, 4H), 7.35 – 7.45 (m, 4H), 7.32 (t, *J* = 7.2 Hz, 1H), 7.22 (t, *J* = 7.2 Hz, 1H), 6.95 - 7.05 (m, 2H), 4.01 (t, *J* = 6.4 Hz, 2H), 3.23 (t, *J* = 6.4 Hz, 2H), 2.03 - 2.13 (m, 2H); >98% @215 nm, MS (ESI) *m/z* = 372.2 [M+H]⁺.

3-(3-(3-phenoxyphenoxy)propyl)-1H-indole-2-carboxylic acid (40)

Coupling of ethyl 3-(3-hydroxypropyl)-1*H*-indole-2-carboxylate and 3-phenoxyphenol yielded **40**. ¹H NMR (400MHz, d₆-DMSO): δ (ppm) 11.42 (s, 1H), 7.61 (d, *J* = 8.4 Hz, 1H), 7.33 – 7.42 (m, 2H), 7.20 – 7.31 (m, 4H), 7.16 (t, *J* = 7.2 Hz, 1H), 6.95 - 7.05 (m, 3H), 6.69 (d, *J* = 7.6 Hz, 1H), 6.52 (s, 1H), 3.93 (t, *J* = 6.4 Hz, 2H), 3.19 (t, *J* = 6.4 Hz, 2H), 1.95 - 2.10 (m, 2H); >98% @215 nm, MS (ESI) *m/z* = 388.2 [M+H]⁺.

3-(3-(4-phenoxyphenoxy)propyl)-1H-indole-2-carboxylic acid (41)

Coupling of ethyl 3-(3-hydroxypropyl)-1*H*-indole-2-carboxylate and 4-phenoxyphenol yielded **41**. ¹H NMR (400MHz, d₆-DMSO): δ (ppm) 11.42 (s, 1H), 7.64 (d, *J* = 8.0 Hz, 1H), 7.32 – 7.45 (m, 3H), 7.23 (t, *J* = 8.0 Hz, 1H), 7.09 (t, *J* = 7.6 Hz, 1H), 6.90 – 7.03 (m, 7H), 3.95 (t, *J* = 6.4 Hz, 2H), 3.21 (t, *J* = 6.8 Hz, 2H), 2.02 – 2.10 (m, 2H); >98% @215 nm, MS (ESI) *m/z* = 388.2 [M+H]⁺.

3-(3-(naphthalen-1-yloxy)propyl)-1H-indole-2-carboxylic acid (42)

Coupling of ethyl 3-(3-hydroxypropyl)-1*H*-indole-2-carboxylate and 1-naphthol yielded **42**. ¹H NMR (400MHz, d₆-DMSO): δ (ppm) 11.60 (s, 1H), 8.24 (d, *J* = 6.8 Hz, 1H), 7.87 (d, *J* = 7.2 Hz, 1H), 7.66 (d, *J* = 8.0 Hz, 1H), 7.30–7.55. (m, 5H), 7.25. (t, *J* = 8.0 Hz, 1H), 6.95 (t, *J* = 7.6 Hz, 1H), 6.87 (d, *J* = 7.6 Hz, 1H), 4.16 (t, *J* = 6.0 Hz, 2H), 3.30 – 3.40 (m, 2H), 2.15 – 2.25 (m, 2H); >98% @215 nm, MS (ESI) *m/z* = 346.1 [M+H]⁺.

3-(3-(naphthalen-2-yloxy)propyl)-1H-indole-2-carboxylic acid (43)

Coupling of ethyl 3-(3-hydroxypropyl)-1*H*-indole-2-carboxylate and 2-naphthol yielded **43**. ¹H NMR (400MHz, d₆-DMSO): δ (ppm) 11.42 (s, 1H), 7.82 (d, *J* = 8.8 Hz, 1H), 7.73 (d, *J* = 8.0 Hz, 1H), 7.67 (d, *J* = 8.0 Hz, 1H), 7.35 – 7.52 (m, 3H), 7.34 (d, *J* = 7.2 Hz, 1H), 7.17 – 7.27 (2H, m), 6.98 (t, *J* = 7.2 Hz, 1H), 4.09 (t, *J* = 6.4 Hz, 2H), 3.26 (t, *J* = 6.4 Hz, 2H), 2.10 – 2.18 (m, 2H); >98% @215 nm, MS (ESI) *m/z* = 346.1 [M+H]⁺.

3-(3-((4-chloronaphthalen-1-yl)oxy)propyl)-1H-indole-2-carboxylic acid (44)

Coupling of ethyl 3-(3-hydroxypropyl)-1*H*-indole-2-carboxylate and 4-chloronaphthalen-1-ol yielded **44**. ¹H NMR (400MHz, d₆-DMSO): δ (ppm) 11.47 (s, 1H), 8.30 (d, *J* = 8.0 Hz, 1H), 8.11 (d, *J* = 8.0 Hz, 1H), 7.73 (t, *J* = 7.2 Hz, 1H), 7.62–7.69 (m, 2H), 7.56 (d, *J* = 8.4 Hz, 1H), 7.40 (d, *J* = 8.4 Hz, 1H), 7.21 (t, *J* = 7.2 Hz, 1H), 6.95 (t, *J* = 7.2 Hz, 1H), 6.88 (d, *J* = 8.4 Hz, 1H), 4.17 (t, *J* = 6.4 Hz, 2H), 3.28 – 2.35 (m, 2H), 2.17 – 2.27 (m, 2H); >98% @215 nm, MS (ESI) *m/z* = 380.1 [M+H]⁺.

3-(3-((5,6,7,8-tetrahydronaphthalen-1-yl)oxy)propyl)-1H-indole-2-carboxylic acid (45)

Coupling of ethyl 3-(3-hydroxypropyl)-1*H*-indole-2-carboxylate and 5,6,7,8-tetrahydronaphthalen-1-ol yielded **45**. ¹H NMR (400MHz, d₆-DMSO): δ (ppm) 11.42 (s, 1H), 7.63 (d, *J* = 8.0 Hz, 1H), 7.40 (d, *J* = 8.0 Hz, 1H), 7.20–7.28 (m, 1H), 6.92–7.07 (m, 2H), 6.60 – 6.70 (m, 2H), 3.94 (t, *J* = 6.4 Hz, 2H), 3.23 (t, *J* = 6.4 Hz, 2H), 2.69 (t, *J* = 0.60 Hz, 2H), 2.63 (t, *J* = 0.60 Hz, 2H), 2.01–2.10 (m, 2H), 1.63 – 1.80 (m, 4H); >98% @215 nm, MS (ESI) *m/z* = 350.2 [M+H]⁺.

3-(3-((2,3-dihydro-1H-inden-5-yl)oxy)propyl)-1H-indole-2-carboxylic acid (46)

Coupling of ethyl 3-(3-hydroxypropyl)-1*H*-indole-2-carboxylate and 2,3-dihydro-1*H*-inden-5-ol yielded **46**. ¹H NMR (400MHz, d₆-DMSO): δ (ppm) 11.42 (s, 1H), 7.64 (d, *J* = 8.0 Hz, 1H), 7.39 (d, *J* = 8.4 Hz, 1H), 7.22 (t, *J* = 7.6 Hz, 1H), 7.08 (d, *J* = 8.4 Hz, 1H), 7.03 (t, *J* = 7.6 Hz, 1H), 6.75 (s, 1H), 6.65 – 6.70 (d, *J* = 8.4 Hz, 1H), 3.91 (t, *J* = 6.4 Hz, 2H), 3.33 (t, *J* = 6.4 Hz, 2H), 2.70 – 2.83 (m, 4H), 1.90 – 2.10 (m, 4H); >98% @215 nm, MS (ESI) *m/z* = 336.1 [M+H]⁺.

3-(3-(quinolin-6-yloxy)propyl)-1H-indole-2-carboxylic acid (47)

Coupling of ethyl 3-(3-hydroxypropyl)-1*H*-indole-2-carboxylate and quinolin-6-ol yielded **47**. ¹H NMR (400MHz, d₆-DMSO): δ (ppm) 11.47 (s, 1H), 8.92 (d, *J* = 4.0 Hz, 1H), 8.53 (d, *J* = 8.0 Hz, 1H), 8.04 (d, *J* = 9.2 Hz, 1H), 7.72 (d, *J* = 8.0 Hz, 1H), 7.66 (d, *J* = 8.0 Hz, 1H), 7.61 (d, *J* = 9.2 Hz, 1H), 7.46 (s, 1H), 7.40 (d, *J* = 8.4 Hz, 1H), 7.61 (d, *J* = 9.2 Hz, 1H), 7.21

(t, $J = 8.0$ Hz, 1H), 6.97 (t, $J = 8.0$ Hz, 1H), 4.14 (t, $J = 6.4$ Hz, 2H), 3.26 (t, $J = 7.2$ Hz, 2H), 2.14-1.93 (m, 2H); >98% @215 nm, MS (ESI) $m/z = 347.1$ [M+H]⁺.

3-(3-((1H-indol-4-yl)oxy)propyl)-1H-indole-2-carboxylic acid (48)

Coupling of ethyl 3-(3-hydroxypropyl)-1*H*-indole-2-carboxylate and quinolin-6-ol yielded **48**. ¹H NMR (400MHz, d₆-DMSO): δ (ppm) 11.45 (s, 1H), 11.04 (s, 1H), 7.68 (d, $J = 8.0$ Hz, 1H), 7.40 (d, $J = 7.8$ Hz, 1H), 7.15-7.30 (m, 2H), 6.91-7.07 (m, 3H), 6.48 (s, 1H), 6.39 (d, $J = 7.2$ Hz, 1H), 4.08 (t, $J = 6.0$ Hz, 2H), 3.26 (t, $J = 6.0$ Hz, 2H), 2.09-2.20 (m, 2H); >98% @215 nm, MS (ESI) $m/z = 335.1$ [M+H]⁺.

4-chloro-3-(3-(4-chloro-3-methylphenoxy)propyl)-1H-indole-2-carboxylic acid (49)

Coupling of ethyl 4-chloro-3-(3-hydroxypropyl)-1*H*-indole-2-carboxylate³⁷ and 4-chloro-3-methylphenol yielded **49**. ¹H NMR (400MHz, d₆-DMSO): δ (ppm) 11.68 (s, 1H), 7.66 (d, $J = 8.4$ Hz, 1H), 7.26 (d, $J = 8.4$ Hz, 1H), 7.19 (t, $J = 8.0$ Hz, 1H), 7.07 (d, $J = 7.6$ Hz, 1H), 6.88-6.94 (m, 1H), 6.69-6.78 (m, 1H), 4.03 (t, $J = 6.4$ Hz, 2H), 3.45 (t, $J = 7.2$ Hz, 2H), 2.27 (s, 3H), 2.01-2.08 (m, 2H); >98% @215 nm, MS (ESI) $m/z = 378.1$ [M+H]⁺.

4-chloro-3-(3-(4-chloro-3,5-dimethylphenoxy)propyl)-1H-indole-2-carboxylic acid (50)

Coupling of ethyl 4-chloro-3-(3-hydroxypropyl)-1*H*-indole-2-carboxylate³⁷ and 4-chloro-3,5-dimethylphenol yielded **50**. ¹H NMR (400MHz, d₆-DMSO): δ (ppm) 11.70 (s, 1H), 7.67 (d, $J = 8.4$ Hz, 1H), 7.19 (t, $J = 7.6$ Hz, 1H), 7.07 (d, $J = 7.6$ Hz, 1H), 6.69 (s, 2H), 4.20 (t, $J = 6.4$ Hz, 2H), 3.44 (t, $J = 7.2$ Hz, 2H), 2.28 (s, 6H), 1.97-2.08 (m, 2H); >98% @215 nm, MS (ESI) $m/z = 392.1$ [M+H]⁺.

4-chloro-3-(3-(naphthalen-1-yloxy)propyl)-1H-indole-2-carboxylic acid (51)

Coupling of ethyl 4-chloro-3-(3-hydroxypropyl)-1*H*-indole-2-carboxylate³⁷ and 1-naphthol yielded **51**. ¹H NMR (400MHz, d₆-DMSO): δ (ppm) 11.68 (s, 1H), 8.18 (d, $J = 8.0$ Hz, 1H), 7.86 (d, $J = 7.6$ Hz, 1H), 7.35-7.57 (m, 5H), 7.21 (d, $J = 8.0$ Hz, 1H), 7.09 (d, $J = 7.2$ Hz, 1H), 6.94 (d, $J = 7.2$ Hz, 1H), 6.69-6.78 (m, $J = 7.2$ Hz, 1H), 4.25 (t, $J = 6.0$ Hz, 2H), 3.60 (t, $J = 7.6$ Hz, 2H), 2.16-2.25 (m, 2H); >98% @215 nm, MS (ESI) $m/z = 380.1$ [M+H]⁺.

6-chloro-3-(3-(4-chloro-3-methylphenoxy)propyl)-1H-indole-2-carboxylic acid (52)

Coupling of ethyl 6-chloro-3-(3-hydroxypropyl)-1*H*-indole-2-carboxylate³⁷ and 4-chloro-3-methylphenol yielded **52**. ¹H NMR (400MHz, d₆-DMSO): δ (ppm) 11.64 (s, 1H), 7.66 (d, $J = 8.8$ Hz, 1H), 7.40 (s, 1H), 7.26 (d, $J = 8.8$ Hz, 1H), 7.02 (d, $J = 6.8$ Hz, 1H), 7.07 (d, $J = 7.6$ Hz, 1H), 6.89 (s, 1H), 6.80 (d, $J = 6.0$ Hz, 1H), 3.93 (t, $J = 6.4$ Hz, 2H), 3.17 (t, $J = 7.2$ Hz, 2H), 2.27 (s, 3H), 1.95-2.08 (m, 2H); >98% @215 nm, MS (ESI) $m/z = 378.1$ [M+H]⁺.

6-chloro-3-(3-(4-chloro-3,5-dimethylphenoxy)propyl)-1H-indole-2-carboxylic acid (53)

Coupling of ethyl 6-chloro-3-(3-hydroxypropyl)-1*H*-indole-2-carboxylate³⁷ and 4-chloro-3,5-dimethylphenol yielded **53**. ¹H NMR (400MHz, d₆-DMSO): δ (ppm) 11.60 (s, 1H), 7.66 (d, $J = 8.4$ Hz, 1H), 7.40 (s, 1H), 7.02 (d, $J = 7.2$ Hz, 1H), 6.73 (s, 2H), 3.92 (t, $J = 6.4$ Hz, 2H), 3.17 (t, $J = 7.6$ Hz, 2H), 2.27 (s, 6H), 1.95-2.05 (m, 2H); >98% @215 nm, MS (ESI) $m/z = 392.1$ [M+H]⁺.

6-chloro-3-(3-(naphthalen-1-yloxy)propyl)-1H-indole-2-carboxylic acid (54)

Coupling of ethyl 6-chloro-3-(3-hydroxypropyl)-1*H*-indole-2-carboxylate³⁷ and 1-naphthol yielded **54**. ¹H NMR (400MHz, d₆-DMSO): δ (ppm) 11.62 (s, 1H), 8.19 (d, $J = 7.6$ Hz, 1H), 7.86 (d, $J = 7.6$ Hz, 1H), 7.69 (d, $J = 8.4$ Hz, 1H), 7.33-7.57 (m, 5H), 6.97 (d, $J = 8.0$ Hz,

1H), 6.87 (d, $J = 8.0$ Hz, 1H), 4.15 (t, $J = 6.4$ Hz, 2H), 3.27-3.37 (m, 2H), 2.16 - 2.25 (m, 2H); >98% @215 nm, MS (ESI) $m/z = 380.1$ [M+H]⁺.

6-chloro-3-(3-((5,6,7,8-tetrahydronaphthalen-1-yl)oxy)propyl)-1H-indole-2-carboxylic acid (55)

Coupling of ethyl 6-chloro-3-(3-hydroxypropyl)-1H-indole-2-carboxylate³⁷ and 5,6,7,8-tetrahydronaphthalen-1-ol yielded **55**. >98% @215 nm, MS (ESI) $m/z = 384.1$ [M+H]⁺.

**3-(3-(4-chloro-3,5-dimethylphenoxy)propyl)-1-methyl-1H-indole-2-carboxylic acid (56):
General Procedure for alkylation of indole NH**

To a solution of ethyl 3-(3-(4-chloro-3,5-dimethylphenoxy)propyl)-1H-indole-2-carboxylate (15 mg, 0.04 mmol) in DMF (0.8 mL) was added NaH (3.0 mg, 0.075 mmol, 60% in mineral oil) at 20 °C under Ar. The reaction mixture was stirred for 20 min at 20 °C then MeI (34 mg, 0.24 mmol) was added. The reaction mixture was stirred for additional 1h then quenched by addition of water. The reaction mixture was extracted with CH₂Cl₂. Combined organic layer was concentrated *in vacuo*, and the residue was purified by reverse phase prep HPLC to give the product as a solid (12 mg, 0.03 mmol). >98% @215 nm, MS (ESI) $m/z = 400.2$ [M+H]⁺.

The title compound was obtained by following the general procedure for saponification outlined above as a white solid. ¹H NMR (400MHz, d₆-DMSO): δ (ppm) 7.67 (d, $J = 8.0$ Hz, 1H), 7.52 (d, $J = 8.0$ Hz, 1H), 7.32 (t, $J = 7.2$ Hz, 1H), 7.07 (t, $J = 7.2$ Hz, 1H), 6.75 (s, 2H), 3.91 - 3.99 (m, 5H), 3.18 (t, $J = 7.2$ Hz, 2H), 2.23 (s, 6H), 1.96 - 2.05 (m, 2H); >98% @215 nm, MS (ESI) $m/z = 372.1$ [M+H]⁺.

Compounds **57 - 59** were prepared following the general procedure outlined above in library format. Purity of all final compounds was determined by HPLC analysis is >95%. All compounds were isolated as solids.

1-methyl-3-(3-(naphthalen-1-yloxy)propyl)-1H-indole-2-carboxylic acid (57)

Methylation of ethyl 3-(3-(naphthalen-1-yloxy)propyl)-1H-indole-2-carboxylate by MeI yielded **57**. ¹H NMR (400MHz, d₆-DMSO): δ 8.22 (d, $J = 6.4$ Hz, 1H), 7.87 (d, $J = 6.4$ Hz, 1H), 7.70 (d, $J = 8.0$ Hz, 1H), 7.36-7.58 (m, 5H), 7.30 (t, $J = 7.6$ Hz, 1H), 7.06 (t, $J = 7.6$ Hz, 1H), 6.87 (d, $J = 7.6$ Hz, 1H), 4.16 (t, $J = 6.0$ Hz, 2H), 3.97 (s, 3H), 3.30 - 3.40 (m, 2H), 2.15 - 2.25 (m, 2H); >98% @215 nm, MS (ESI) $m/z = 360.1$ [M+H]⁺.

6-Chloro-3-(3-(4-chloro-3,5-dimethylphenoxy)propyl)-1-methyl-1H-indole-2-carboxylic acid (58)

Methylation of ethyl 6-chloro-3-(3-(4-chloro-3,5-dimethylphenoxy)propyl)-1H-indole-2-carboxylate by MeI yielded **58**. ¹H NMR (400MHz, d₆-DMSO): δ 7.79-7.57 (m, 2H), 7.07 (dd, $J = 8.6, 1.7$ Hz, 1H), 6.73 (s, 2H), 3.97-3.89 (m, 5H), 3.20-3.10 (m, 2H), 2.27 (s, 6H), 2.06-1.93 (m, 2H); >98% @215 nm, MS (ESI) 1.83 min, $m/z = 428$ [M+Na]⁺.

1-benzyl-3-(3-(naphthalen-1-yloxy)propyl)-1H-indole-2-carboxylic acid (59)

Benylation of ethyl 3-(3-(naphthalen-1-yloxy)propyl)-1H-indole-2-carboxylate by and benzyl bromide yielded **59**. ¹H NMR (400MHz, d₆-DMSO): δ (ppm) 8.18 - 8.24 (m, 1H), 7.87 (d, $J = 7.2$ Hz, 1H), 7.72-7.80 (m, 1H), 7.42 - 7.56 (m, 3H), 7.35 - 7.40 (m, 1H), 7.15 - 7.30 (m, 5H), 6.95 - 7.10 (m, 3H), 6.83 - 6.90 (m, 1H), 5.84 (s, 2H), 4.17 (t, $J = 6.0$ Hz, 2H), 3.30 - 3.40 (m, 2H), 2.15 - 2.25 (m, 2H); >98% @215 nm, MS (ESI) $m/z = 436.2$ [M+H]⁺.

1-(3-(4-chloro-3-methylphenoxy)propyl)-1H-indole-2-carboxylic acid (69)

The title compound was obtained by following the general procedure for phenol analogue coupling and saponification outlined above using ethyl 1-(3-hydroxypropyl)-1H-indole-2-carboxylate and 4-chloro-3-methylphenol as a white solid. >98% @215 nm, MS (ESI) $m/z = 344.1 [M+H]^+$.

1-(3-(4-chloro-3,5-dimethylphenoxy)propyl)-1H-indole-2-carboxylic acid (70)

The title compound was obtained by following the general procedure for phenol analogue coupling and saponification outlined above using ethyl 1-(3-hydroxypropyl)-1H-indole-2-carboxylate and 4-chloro-3,5-dimethylphenol as a white solid. >98% @215 nm, MS (ESI) $m/z = 357.1 [M+H]^+$.

1-(3-(naphthalen-1-yloxy)propyl)-1H-indole-2-carboxylic acid (71)

The title compound was obtained by following the general procedure for phenol analogue coupling and saponification outlined above using ethyl 1-(3-hydroxypropyl)-1H-indole-2-carboxylate and 1-naphthol as a white solid. $^1\text{H NMR}$ (400MHz, d_6 -DMSO): δ (ppm) 8.26 (d, $J = 7.2$ Hz, 1H), 7.87 (d, $J = 7.2$ Hz, 1H), 7.69 (d, $J = 8.0$ Hz, 1H), 7.37-7.57. (m, 4H), 7.35 (t, $J = 8.0$ Hz, 1H), 7.15-7.25 (m, 2H), 7.07. (t, $J = 7.2$ Hz, 1H), 6.85 (d, $J = 7.2$ Hz, 1H), 4.89 (t, $J = 6.8$ Hz, 2H), 4.23 (t, $J = 7.2$ Hz, 2H), 2.15 - 2.25 (m, 2H); >98% @215 nm, MS (ESI) $m/z = 346.1 [M+H]^+$.

1-(3-(naphthalen-1-yloxy)propyl)-1H-indole-2-carboxamide (72)

To a solution of 1-(3-(naphthalen-1-yloxy)propyl)-1H-indole-2-carboxylic acid (15 mg, 0.043 mmol) in CH_2Cl_2 (1.0 mL) was added oxalyl chloride (37 μL , 0.43 mmol) followed by a drop of N,N -dimethylformamide at room temperature under Ar. The reaction mixture was stirred for 3 h at room temperature then concentrated under vacuum. The residue was re-dissolved in CH_2Cl_2 (0.5 ml) and conc. NH_4OH aqueous solution (0.67 ml) was added. The reaction mixture was stirred for 2 h then extracted with ethyl acetate. The organic layer was concentrated *in vacuo*, and the residue was purified by reverse phase prep HPLC to give the product as a white solid (11 mg, 0.032 mmol). $^1\text{H NMR}$ (400MHz, d_6 -DMSO): δ (ppm) 8.24 - 8.30 (m, 1H), 7.99 (br, 2H), 7.82 - 7.90 (m, 1H), 7.63 (d, $J = 8.0$, 1H), 7.47 - 7.60 (m, 3H), 7.42 - 7.46 (m, 1H), 7.35 - 7.40. (m, 1H), 7.19 (s, 1H), 7.14 (t, $J = 7.2$ Hz, 1H), 7.06 (t, $J = 7.2$ Hz, 1H), 6.84 (t, $J = 7.2$ Hz, 1H), 4.86 (t, $J = 7.2$ Hz, 2H), 4.12 (t, $J = 6.0$ Hz, 2H), 2.25 - 2.35 (m, 2H); >98% @215 nm, MS (ESI) $m/z = 345.1 [M+H]^+$.

Supplementary Material

Refer to Web version on PubMed Central for supplementary material.

Acknowledgments

The authors thank co-workers at the High-Throughput Screening Core facility of Vanderbilt University for compound management and providing the instrumentation to perform the binding assay and Dr. Olivia Rossanese for critical reading of the manuscript. The pDEST-HisMBP entry plasmid and a TEV protease expression vector were kindly provided by Dr. David S. Waugh (National Cancer Institute) and Dr. Arie Geerlof (Helmholz Zentrum München, Germany), respectively.

This research was supported by the US National Institutes of Health: NIH Director's Pioneer Award (DP1OD006933/DP1CA174419) to S.W.F., an ARRA stimulus grant (RC2A148375) to L. J. Marnett, and a career development award to S.W.F. from a NCI SPORE grant in breast cancer (P50CA098131) to C. L. Arteaga. This work was also funded by the American Cancer Society (Postdoctoral Fellowship, PF1110501CDD) to J.P.B.

The Biomolecular NMR Facility at Vanderbilt University is supported in part by a NIH SIG grant (#1S-10RR025677-01) and Vanderbilt University matching funds. Use of the Advanced Photon Source was

supported by the U. S. Department of Energy, Office of Science, Office of Basic Energy Sciences, under Contract No. DE-AC02-06CH11357. Use of the LS-CAT Sector 21 was supported by the Michigan Economic Development Corporation and the Michigan Technology Tri-Corridor for the support of this research program (Grant 085P1000817).

ABBREVIATIONS

FBDD	fragment-based drug discovery
Mcl-1	Myeloid cell leukemia 1
Bcl-2	B-cell lymphoma 2
Bcl-xL	B-cell lymphoma-extra large
BH3	Bcl-2 homology domain 3
CSP	chemical shift perturbation
FITC	fluorescein isothiocyanate
FPA	fluorescence polarization anisotropy

REFERENCES

- (1). Danial NN, Korsmeyer SJ. Cell death: critical control points. *Cell*. 2004; 116:205–219. [PubMed: 14744432]
- (2). Adams JM, Cory S. The Bcl-2 apoptotic switch in cancer development and therapy. *Oncogene*. 2007; 26:1324–1337. [PubMed: 17322918]
- (3). Willis SN, Fletcher JI, Kaufmann T, van Delft MF, Chen L, Czabotar PE, Ierino H, Lee EF, Fairlie WD, Bouillet P, Strasser A, Kluck RM, Adams JM, Huang DCS. Apoptosis initiated when BH3 ligands engage multiple Bcl-2 homologs, not Bax or Bak. *Science*. 2007; 315:856–859. [PubMed: 17289999]
- (4). Beroukhim R, Mermel CH, Porter D, Wei G, Raychaudhuri S, Donovan J, Barretina J, Boehm JS, Dobson J, Urashima M, Mc Henry KT, Pinchback RM, Ligon AH, Cho Y-J, Haery L, Greulich H, Reich M, Winckler W, Lawrence MS, Weir BA, Tanaka KE, Chiang DY, Bass AJ, Loo A, Hoffman C, Prensner J, Liefeld T, Gao Q, Yecies D, Signoretti S, Maher E, Kaye FJ, Sasaki H, Tepper JE, Fletcher JA, Taberner J, Baselga J, Tsao M-S, Demichelis F, Rubin MA, Janne PA, Daly MJ, Nucera C, Levine RL, Ebert BL, Gabriel S, Rustgi AK, Antonescu CR, Ladanyi M, Letai A, Garraway LA, Loda M, Beer DG, True LD, Okamoto A, Pomeroy SL, Singer S, Golub TR, Lander ES, Getz G, Sellers WR, Meyerson M. The landscape of somatic copy-number alteration across human cancers. *Nature*. 2010; 463:899–905. [PubMed: 20164920]
- (5). Wei G, Margolin AA, Haery L, Brown E, Cucolo L, Julian B, Shehata S, Kung AL, Beroukhim R, Golub TR. Chemical genomics identifies small-molecule MCL1 repressors and BCL-xL as a predictor of MCL1 dependency. *Cancer Cell*. 2012; 21:547–562. [PubMed: 22516262]
- (6). Song L, Coppola D, Livingston S, Cress D, Haura EB. Mcl-1 regulates survival and sensitivity to diverse apoptotic stimuli in human non-small cell lung cancer cells. *Cancer Biol. Ther.* 2005; 4:267–276. [PubMed: 15753661]
- (7). Ding Q, He X, Xia W, Hsu J-M, Chen C-T, Li L-Y, Lee D-F, Yang J-Y, Xie X, Liu J-C, Hung M-C. Myeloid cell leukemia-1 inversely correlates with glycogen synthase kinase-3beta activity and associates with poor prognosis in human breast cancer. *Cancer Res.* 2007; 67:4564–4571. [PubMed: 17495324]
- (8). Krajewska M, Krajewski S, Epstein JI, Shabaik A, Sauvageot J, Song K, Kitada S, Reed JC. Immunohistochemical analysis of bcl-2, bax, bcl-X, and mcl-1 expression in prostate cancers. *Am. J. Pathol.* 1996; 148:1567–1576. [PubMed: 8623925]
- (9). Miyamoto Y, Hosotani R, Wada M, Lee JU, Koshihara T, Fujimoto K, Tsuji S, Nakajima S, Doi R, Kato M, Shimada Y, Imamura M. Immunohistochemical analysis of Bcl-2, Bax, Bcl-X, and Mcl-1 expression in pancreatic cancers. *Oncology.* 1999; 56:73–82. [PubMed: 9885381]

- (10). Brotin E, Meryet-Figuière M, Simonin K, Duval RE, Villedieu M, Leroy-Dudal J, Saison-Behmoaras E, Gauduchon P, Denoyelle C, Poulain L. Bcl-XL and MCL-1 constitute pertinent targets in ovarian carcinoma and their concomitant inhibition is sufficient to induce apoptosis. *Int. J. Cancer.* 2010; 126:885–895. [PubMed: 19634140]
- (11). Derenne S, Monia B, Dean NM, Taylor JK, Rapp M-J, Harousseau J-L, Bataille R, Amiot M. Antisense strategy shows that Mcl-1 rather than Bcl-2 or Bcl-x(L) is an essential survival protein of human myeloma cells. *Blood.* 2002; 100:194–199. [PubMed: 12070027]
- (12). Andersen MH, Becker JC, Thor Straten P. The antiapoptotic member of the Bcl-2 family Mcl-1 is a CTL target in cancer patients. *Leukemia.* 2005; 19:484–485. [PubMed: 15618955]
- (13). Kang MH, Wan Z, Kang YH, Sposto R, Reynolds CP. Mechanism of synergy of N-(4-hydroxyphenyl)retinamide and ABT-737 in acute lymphoblastic leukemia cell lines: Mcl-1 inactivation. *J. Natl. Cancer Inst.* 2008; 100:580–595. [PubMed: 18398104]
- (14). Wertz IE, Kusam S, Lam C, Okamoto T, Sandoval W, Anderson DJ, Helgason E, Ernst JA, Eby M, Liu J, Belmont LD, Kaminker JS, O'Rourke KM, Pujara K, Kohli PB, Johnson AR, Chiu ML, Lill JR, Jackson PK, Fairbrother WJ, Seshagiri S, Ludlam MJC, Leong KG, Dueber EC, Maecker H, Huang DCS, Dixit VM. Sensitivity to antitubulin chemotherapeutics is regulated by MCL1 and FBW7. *Nature.* 2011; 471:110–114. [PubMed: 21368834]
- (15). Wei S-H, Dong K, Lin F, Wang X, Li B, Shen J-J, Zhang Q, Wang R, Zhang H-Z. Inducing apoptosis and enhancing chemosensitivity to gemcitabine via RNA interference targeting Mcl-1 gene in pancreatic carcinoma cell. *Cancer Chemother. Pharmacol.* 2008; 62:1055–1064. [PubMed: 18297287]
- (16). van Delft MF, Wei AH, Mason KD, Vandenberg CJ, Chen L, Czabotar PE, Willis SN, Scott CL, Day CL, Cory S, Adams JM, Roberts AW, Huang DCS. The BH3 mimetic ABT-737 targets selective Bcl-2 proteins and efficiently induces apoptosis via Bak/Bax if Mcl-1 is neutralized. *Cancer Cell.* 2006; 10:389–399. [PubMed: 17097561]
- (17). Varin E, Denoyelle C, Brotin E, Meryet-Figuière M, Giffard F, Abeilard E, Goux D, Gauduchon P, Icard P, Poulain L. Downregulation of Bcl-xL and Mcl-1 is sufficient to induce cell death in mesothelioma cells highly refractory to conventional chemotherapy. *Carcinogenesis.* 2010; 31:984–993. [PubMed: 20142415]
- (18). Olberding KE, Wang X, Zhu Y, Pan J, Rai SN, Li C. Actinomycin D synergistically enhances the efficacy of the BH3 mimetic ABT-737 by downregulating Mcl-1 expression. *Cancer Biol. Ther.* 2010; 10:918–929. [PubMed: 20818182]
- (19). Zhang H, Guttikonda S, Roberts L, Uziel T, Semizarov D, Elmore SW, Levenson JD, Lam LT. Mcl-1 is critical for survival in a subgroup of non-small-cell lung cancer cell lines. *Oncogene.* 2011; 30:1963–1968. [PubMed: 21132008]
- (20). Rega MF, Wu B, Wei J, Zhang Z, Cellitti JF, Pellecchia M. SAR by interligand nuclear overhauser effects (ILOEs) based discovery of acylsulfonamide compounds active against Bcl-x(L) and Mcl-1. *J. Med. Chem.* 2011; 54:6000–6013. [PubMed: 21797225]
- (21). Cohen NA, Stewart ML, Gavathiotis E, Tepper JL, Bruekner SR, Koss B, Opferman JT, Walensky LD. A Competitive Stapled Peptide Screen Identifies a Selective Small Molecule that Overcomes MCL-1-Dependent Leukemia Cell Survival. *Chemistry & Biology.* 2012; 19:1175–1186. [PubMed: 22999885]
- (22). Kim YB, Balasis ME, Doi K, Berndt N, Duboulay C, Hu C-CA, Guida W, Wang H-G, Sebti SM, Del Valle JR. Synthesis and evaluation of substituted hexahydronaphthalenes as novel inhibitors of the Mcl-1/BimBH3 interaction. *Bioorg. Med. Chem. Lett.* 2012; 22:5961–5965. [PubMed: 22901384]
- (23). Stewart ML, Fire E, Keating AE, Walensky LD. The MCL-1 BH3 helix is an exclusive MCL-1 inhibitor and apoptosis sensitizer. *Nat. Chem. Biol.* 2010; 6:595–601. [PubMed: 20562877]
- (24). Muppidi A, Doi K, Edwardraja S, Drake EJ, Gulick AM, Wang H-G, Lin Q. Rational Design of Proteolytically Stable, Cell-Permeable Peptide-Based Selective Mcl-1 Inhibitors. *J. Am. Chem. Soc.* 2012; 134:14734–14737. [PubMed: 22920569]
- (25). Shuker SB, Hajduk PJ, Meadows RP, Fesik SW. Discovering high-affinity ligands for proteins: SAR by NMR. *Science.* 1996; 274:1531–1534.

- (26). Murray CW, Blundell TL. Structural biology in fragment-based drug design. *Curr. Opin. Struct. Biol.* 2010; 20:497–507.
- (27). Oltersdorf T, Elmore SW, Shoemaker AR, Armstrong RC, Augeri DJ, Belli BA, Bruncko M, Deckwerth TL, Dinges J, Hajduk PJ, Joseph MK, Kitada S, Korsmeyer SJ, Kunzer AR, Letai A, Li C, Mitten MJ, Nettesheim DG, Ng S, Nimmer PM, O'Connor JM, Oleksijew A, Petros AM, Reed JC, Shen W, Tahir SK, Thompson CB, Tomaselli KJ, Wang B, Wendt MD, Zhang H, Fesik SW, Rosenberg SH. An inhibitor of Bcl-2 family proteins induces regression of solid tumours. *Nature.* 2005; 435:677–681. [PubMed: 15902208]
- (28). Tse C, Shoemaker AR, Adickes J, Anderson MG, Chen J, Jin S, Johnson EF, Marsh KC, Mitten MJ, Nimmer P, Roberts L, Tahir SK, Xiao Y, Yang X, Zhang H, Fesik S, Rosenberg SH, Elmore SW. ABT-263: a potent and orally bioavailable Bcl-2 family inhibitor. *Cancer Res.* 2008; 68:3421–3428. [PubMed: 18451170]
- (29). Huth JR, Park C, Petros AM, Kunzer AR, Wendt MD, Wang X, Lynch CL, Mack JC, Swift KM, Judge R. a, Chen J, Richardson PL, Jin S, Tahir SK, Matayoshi ED, Dorwin S. a, Lador US, Severin JM, Walter K. a, Bartley DM, Fesik SW, Elmore SW, Hajduk PJ. Discovery and design of novel HSP90 inhibitors using multiple fragment-based design strategies. *Chem Biol Drug Des.* 2007; 70:1–12. [PubMed: 17630989]
- (30). Wyss DF, Wang Y-S, Eaton HL, Strickland C, Voigt JH, Zhu Z, Stamford AW. Combining NMR and X-ray crystallography in fragment-based drug discovery: discovery of highly potent and selective BACE-1 inhibitors. *Top Curr Chem.* 2012; 317:83–114. [PubMed: 21647837]
- (31). Kuntz ID, Chen K, Sharp KA, Kollman PA. The maximal affinity of ligands. *Proc. Natl. Acad. Sci. U.S.A.* 1999; 96:9997–10002. [PubMed: 10468550]
- (32). Murray CW, Rees DC. The rise of fragment-based drug discovery. *Nat Chem.* 2009; 1:187–192. [PubMed: 21378847]
- (33). Bruncko M, Song X, Ding H, Tao Z-F, Kunzer AR. 7-Nonsubstituted indoles as Mcl-1 inhibitors and their preparation. *PCT Int. Appl.* 2008:WO–0130970–A1.
- (34). Elmore SW, Souers AJ, Bruncko M, Song X, Wang X, Hasvold LA, Wang L, Kunzer AR, Park C-M, Wendt MD, Tao Z-F. 7-Substituted indoles as Mcl-1 protein inhibitors and their preparation. *PCT Int. Appl.* 2008:WO–0131000–A2.
- (35). Fire E, Gullá SV, Grant RA, Keating AE. Mcl-1-Bim complexes accommodate surprising point mutations via minor structural changes. *Protein Sci.* 2010; 19:507–519. [PubMed: 20066663]
- (36). Petros AM, Olejniczak ET, Fesik SW. Structural biology of the Bcl-2 family of proteins. *Biochim. Biophys. Acta.* 2004; 1644:83–94. [PubMed: 14996493]
- (37). Salituro FG, Harrison BL, Baron BM, Nyce PL, Stewart KT, McDonald IA. 3-(2-carboxyindol-3-yl)propionic acid derivatives: antagonists of the strychnine-insensitive glycine receptor associated with the N-methyl-D-aspartate receptor complex. *J. Med. Chem.* 1990; 33:2944–2946. [PubMed: 2146391]
- (38). Konopleva M, Contractor R, Tsao T, Samudio I, Ruvolo PP, Kitada S, Deng X, Zhai D, Shi Y-X, Sneed T, Verhaegen M, Soengas M, Ruvolo VR, McQueen T, Schober WD, Watt JC, Jiffar T, Ling X, Marini FC, Harris D, Dietrich M, Estrov Z, McCubrey J, May WS, Reed JC, Andreeff M. Mechanisms of apoptosis sensitivity and resistance to the BH3 mimetic ABT-737 in acute myeloid leukemia. *Cancer Cell.* 2006; 10:375–388. [PubMed: 17097560]
- (39). Schanda P, Brutscher B. Very fast two-dimensional NMR spectroscopy for real-time investigation of dynamic events in proteins on the time scale of seconds. *J. Am. Chem. Soc.* 2005; 127:8014–8015. [PubMed: 15926816]
- (40). Congreve M, Carr R, Murray C, Jhoti H. A “rule of three” for fragment-based lead discovery? *Drug Discov. Today.* 2003; 8:876–877. [PubMed: 14554012]
- (41). Sattler M, Schleucher J, Griesinger C. Heteronuclear multidimensional NMR experiments for the structure determination of proteins in solution employing pulsed. *Progress in Nuclear Magnetic Resonance Spectroscopy.* 1999; 34:93–158.
- (42). Schwieters CD, Kuszewski JJ, Tjandra N, Clore GM. The Xplor-NIH NMR molecular structure determination package. *J Magn Reson.* 2003; 160:65–73. [PubMed: 12565051]

- (43). Otwinowski, Z.; Minor, W. Processing of X-ray diffraction data collected in oscillation mode. In: Carter, Charles W.; J. B., T-M.; E., editors. *Macromolecular Crystallography Part A*. Vol. Volume 276. Academic Press; 1997. p. 307-326.
- (44). McCoy AJ, Grosse-Kunstleve RW, Adams PD, Winn MD, Storoni LC, Read RJ. Phaser crystallographic software. *Journal of Applied Crystallography*. 2007; 40:658–674. [PubMed: 19461840]
- (45). Winn MD, Ballard CC, Cowtan KD, Dodson EJ, Emsley P, Evans PR, Keegan RM, Krissinel EB, Leslie AGW, McCoy A, McNicholas SJ, Murshudov GN, Pannu NS, Potterton EA, Powell HR, Read RJ, Vagin A, Wilson KS. Overview of the CCP4 suite and current developments. *Acta Crystallogr. D Biol. Crystallogr.* 2011; 67:235–242. [PubMed: 21460441]
- (46). Adams PD, Grosse-Kunstleve RW, Hung LW, Ioerger TR, McCoy AJ, Moriarty NW, Read RJ, Sacchettini JC, Sauter NK, Terwilliger TC. PHENIX: building new software for automated crystallographic structure determination. *Acta Crystallogr D Biol Crystallogr.* 2002; 58:1948–1954. [PubMed: 12393927]
- (47). Murshudov GN, Skubák P, Lebedev AA, Pannu NS, Steiner RA, Nicholls RA, Winn MD, Long F, Vagin AA. REFMAC5 for the refinement of macromolecular crystal structures. *Acta Crystallogr. D Biol. Crystallogr.* 2011; 67:355–367. [PubMed: 21460454]
- (48). Emsley P, Cowtan K. Coot: model-building tools for molecular graphics. *Acta Crystallogr D Biol Crystallogr.* 2004; 60:2126–2132. [PubMed: 15572765]
- (49). Schrödinger, L. The PyMOL Molecular Graphics System, Version 1.5. 2010.
- (50). Wang ZX, Jiang RF. A novel two-site binding equation presented in terms of the total ligand concentration. *FEBS Lett.* 1996; 392:245–249. [PubMed: 8774854]
- (51). Piemontese L, Carbonara G, Fracchiolla G, Laghezza A, Tortorella P, Loiodice F. Convenient Synthesis of Some 3-Phenyl-1-benzofuran-2-carboxylic Acid Derivatives as New Potential Inhibitors of CLC-Kb Channels. *Heterocycles.* 2010; 81:2865–2872.
- (52). Laskowski R, MacArthur M, Moss D, Thornton J. PROCHECK: a program to check the stereochemical quality of protein structures. *J. Appl. Cryst.* 1993; 26:283–291.

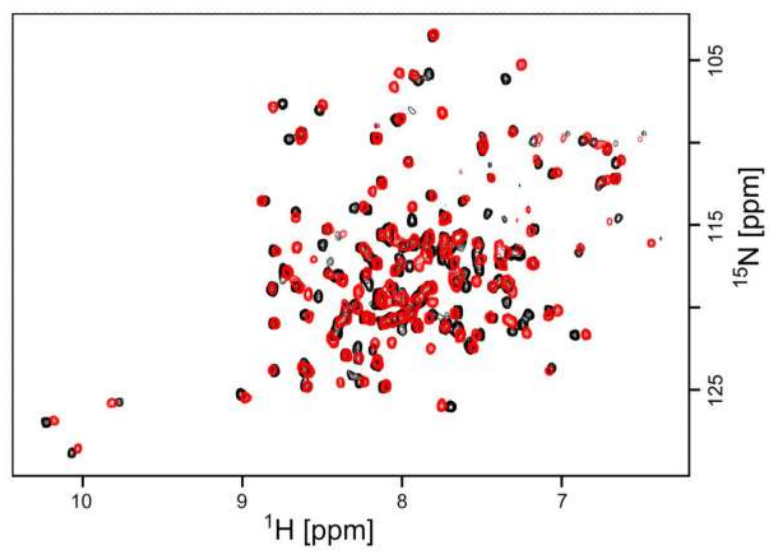


Figure 1. ^1H - ^{15}N HMQC spectra of Mcl-1 with (red) and without (black) fragment **3**. The NMR sample contained $50\mu\text{M}$ ^{15}N -labeled protein and 800HM ligand.

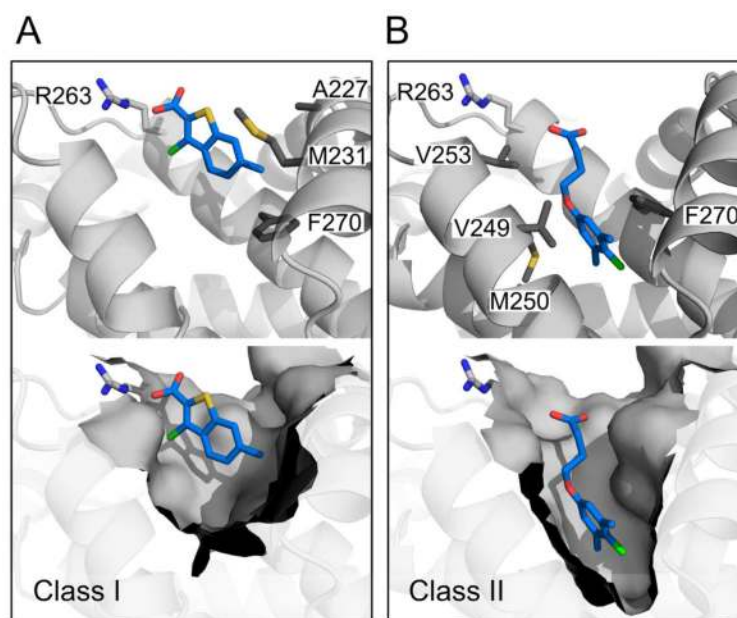


Figure 2. Model structures of Mcl-1 complexed to two different classes of fragment hits obtained using NMR-derived distance restraints. Residues (labeled) with NOEs to the fragments (blue) are rendered as sticks (gray). R263 is also labeled. (A) Class I: benzothiophene **5**, and (B) Class II: tethered aromatic **17**.

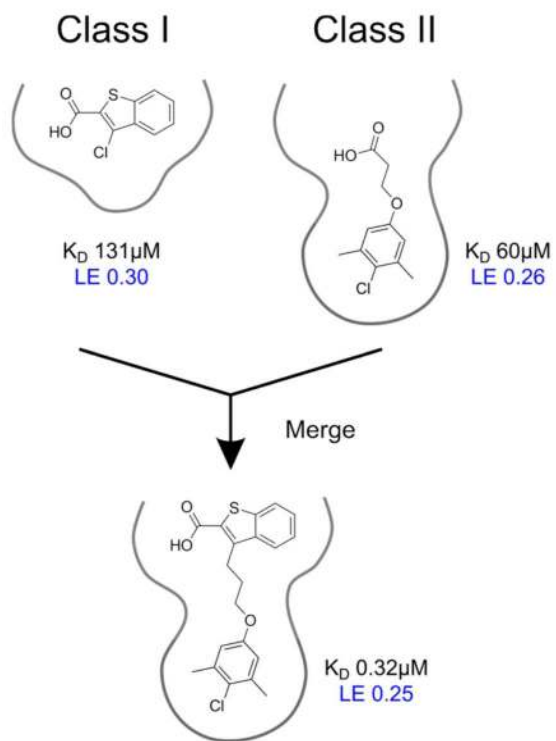


Figure 3. Schematic illustrating the merging of fragment **2** and **17** to produce compound **60**. The affinity of each molecule to Mcl-1 is shown as well as the ligand efficiencies.

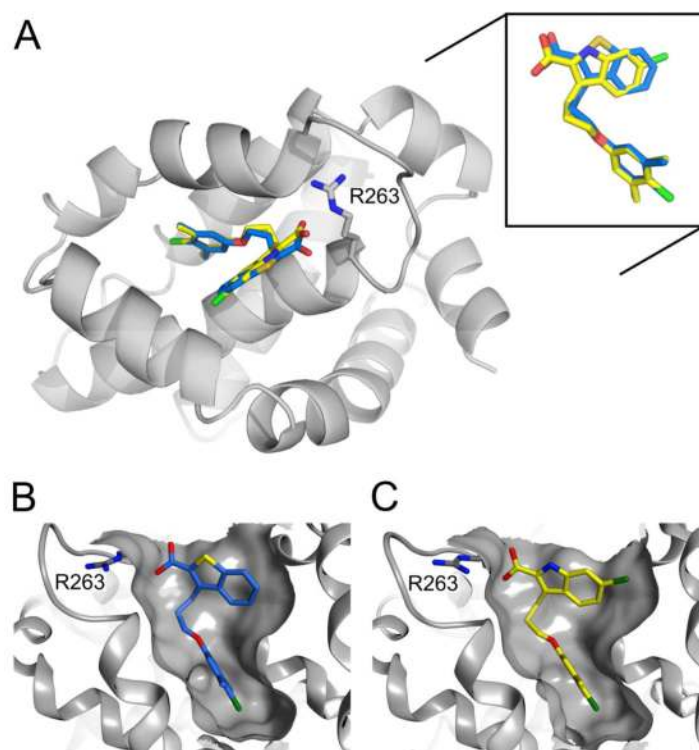


Figure 4. X-ray structures of merged compounds bound to Mcl-1. Compounds incorporating different scaffolds (benzothiophene and indole) occupy the same binding pocket and adopt very similar binding poses (inset). (A) Compounds **53** and **60** interact with Mcl-1 in the BH3-peptide binding cleft between helices 3, 4, and 5. Surface depiction of Mcl-1 when complexed to (B) **60** and (C) **53** that illustrates how the merged compounds fill the pockets as predicted by NMR and interact with R263.

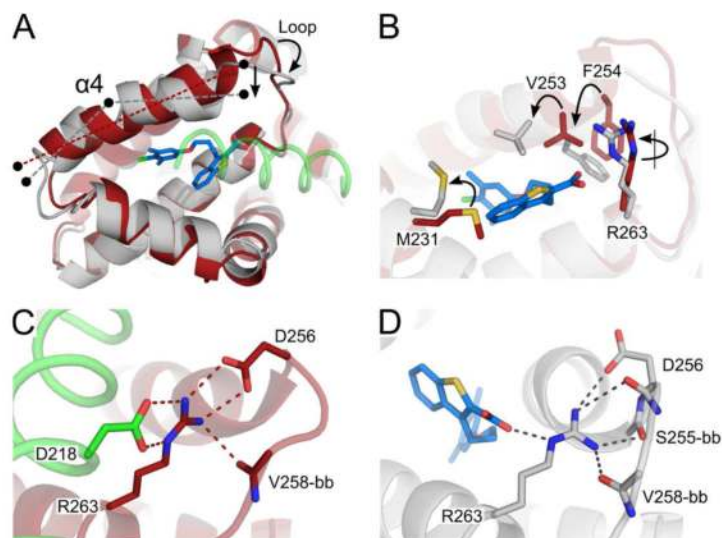


Figure 5.

Several structural differences between peptide-bound (red) and compound-bound (gray) Mcl-1 complexes were identified. The Mcl-1-derived BH3-peptide is depicted in green and compound **60** in blue. (A) To accommodate the hydrophobic fragments into the deep pocket, helix 4 ($\alpha 4$) is slightly kinked in the structures of Mcl-1/compound complexes compared to the Mcl-1/peptide structures. This leads to further rearrangements of the loop, pulling it towards the merged compound. (B) Close-up of the small-molecule binding-site in Mcl-1. Compared to the peptide-bound state, our merged compounds induce changes in the position and/or in rotamer states of nearby residues. (C-D) The network of charge-charge interactions and polar contacts involving R263 are dramatically different in the two types of complexes. (C) While bound to the peptide, R263 of Mcl-1 interacts closely with D218 of the 16mer, a residue shown important by alanine-scanning.²³ Moreover, R263 interacts with the side-chain of D256 and the backbone (bb) oxygen of V258 in Mcl-1. (D) When complexed with merged compounds (e.g. **60**), this network is replaced by an interaction to the carboxylic acid of the small-molecule ligand and additional polar contacts to the backbone oxygen atoms of S255 and D256.

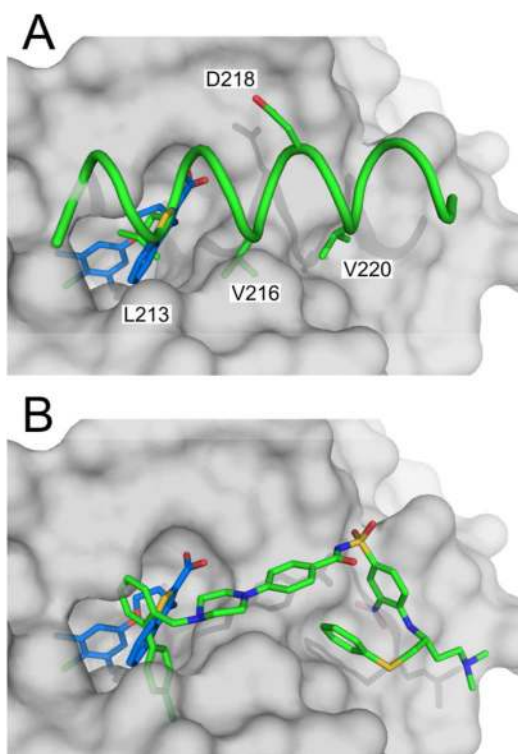
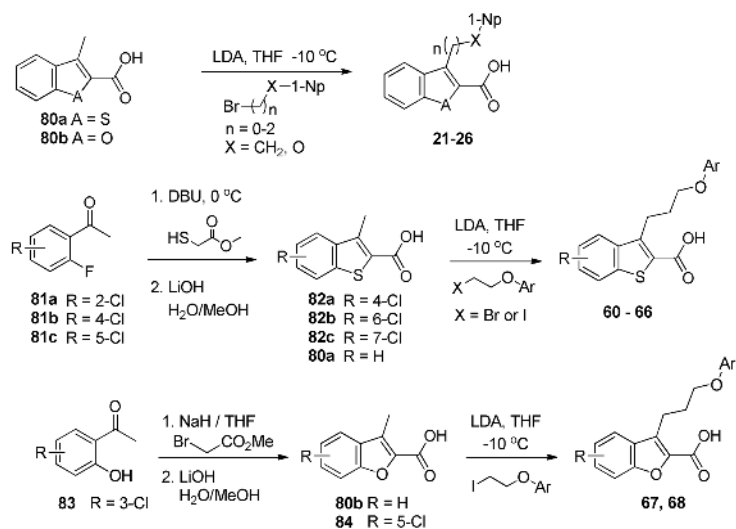
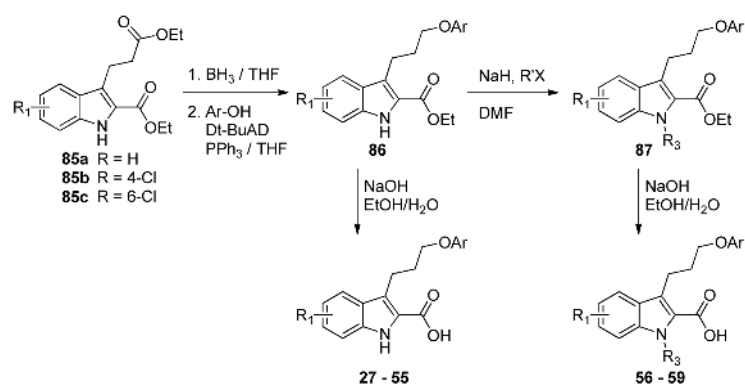


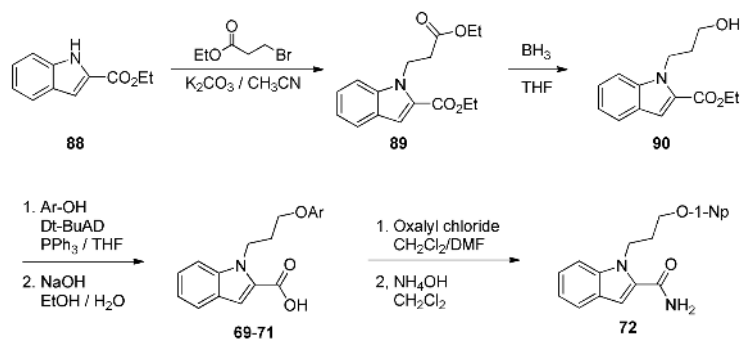
Figure 6. (A) Comparison of Mcl-1 (gray surface) when complexed to compound **60** (blue) and a 16mer BH3-peptide derived from Mcl-1 (green), (B) Overlay of the X-ray structures of Mcl-1/**60** complex and Bcl-xL/ABT-737 (PDB: 2YXJ). The Mcl-1 protein is shown in gray, **60** in blue, and ABT-737 in green.



Scheme 1.
 Synthesis of benzothiophene- and benzofuran-containing compounds



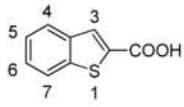
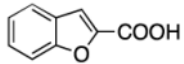
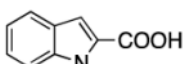
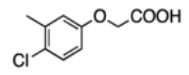
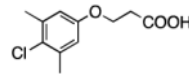
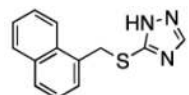
Scheme 2.
Synthesis of indole-based compounds



Scheme 3.
Synthesis of compounds 69-72

Table 1

SAR of Class I and II fragment hits for binding to Bcl-2 family proteins

Class I						
Structure	Comp. Substitutions	K _i (μM)*			LE (Mcl-1)	
		Mcl-1	Bcl-xL	Bcl-2		
	1	H	>1000			
	2	3-Cl	131		0.30	
	3	3-Cl, 4-Cl	22	>1000	>1000	0.33
	4	3-Cl, 6-Cl	59			0.30
	5	3-Cl, 6-Me	40	230	>1000	0.31
	6	H	>1000			
	7	3-Me, 5-Cl	52		0.31	
	8	3-Me, 6-Cl	23		0.33	
	9	3-Me, 7-Me	102	>1000	>1000	0.29
	10	3-Me, 6-Me, 7-Me	214	>1000	>1000	0.24
	11	4-Br, 6-Cl	90		0.29	
	12	H	>1000			
	13	1-Me	160		0.29	
	14	1-Me, 5-Br	81		0.29	
	15	3-Ph, 7-Me	136	>1000	>1000	0.20
	Class II					
Comp.	Structure	K _i (μM)*			LE (Mcl-1)	
		Mcl-1	Bcl-xL	Bcl-2		
16		103	>1000	>1000	0.31	
17		60	>1000	>1000	0.26	
18		86	>1000	>1000	0.24	

* K_i values are measured in duplicate and average values are reported.

Analogs from the Vanderbilt compound library

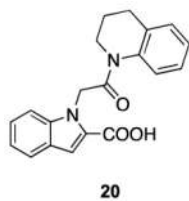
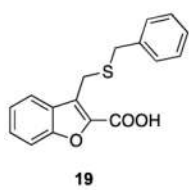
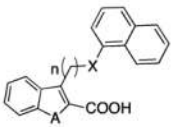


Table 2

Optimization of linker length in the merged compounds

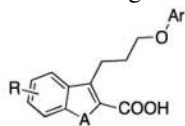


Comp.	A	n	X	K _i (μM)		
				Mcl-1 ^a	Bcl-xL ^b	Bcl-2 ^b
21	S	1	CH ₂	12.5 ± 5.6		
22	S	2	CH ₂	9.6 ± 3.0		
23	S	3	O	0.37 ± 0.03	15	9.7
24	O	1	CH ₂	9.5 ± 2.9		
25	O	2	CH ₂	14.6 ± 7.1		
26	O	3	O	1.0 ± 0.44	>15	4.3

^aK_i values are measured in triplicate^bK_i values are measured in duplicate

Table 3

SAR of merged compounds containing an optimized 4-atom linker



Comp.	A	R	Ar	K _i (μM)		
				Mcl-1 ^a	Bcl-xL ^b	Bcl-2 ^b
27	NH	H	Ph	35 ± 7.1		
28	NH	H	2-Me-Phenyl	15 ± 0.7		
29	NH	H	2-CF ₃ -Phenyl	8.8 ± 1.7		
30	NH	H	3-Me-Phenyl	1.9 ± 0.6		
31	NH	H	3-CF ₃ -Phenyl	1.7 ± 0.08		
32	NH	H	4-Me-Phenyl	16 ± 3.1		
33	NH	H	4-Cl-Phenyl	9.8 ± 2.9		
34	NH	H	4-CF ₃ -Phenyl	9.9 ± 3.2		
35	NH	H	3-Me-4-Cl-Phenyl	0.38 ± 0.14	>15	9.1
36	NH	H	3-Et-4-Cl-Phenyl	1.1 ± 0.1		
37	NH	H	3,5-diMe-4-Cl-Phenyl	0.30 ± 0.15	>15	5.3
38	NH	H	3-(1,1'-biphenyl)	7.7 ± 2.1		
39	NH	H	4-(1,1'-biphenyl)	7.6 ± 0.7		
40	NH	H	3-Phenoxy-Phenyl	5.2 ± 0.3		
41	NH	H	4-Phenoxy-Phenyl	6.4 ± 0.6		
42	NH	H	1-Naphthyl	0.33 ± 0.10	>15	2.7
43	NH	H	2-Naphthyl	7.5 ± 0.6		
44	NH	H	1-(4-Cl-Naphthyl)	0.48 ± 0.01		
45	NH	H	1-(5,6,7,8-tetrahydronaphthyl)	0.30 ± 0.10		
46	NH	H	5-(2,3-dihydroindenyl)	2.9 ± 0.1		
47	NH	H	6-Quinoliny	62 ± 17		
48	NH	H	4-Indolyl	14 ± 0.3		
49	NH	4-Cl	3-Me-4-Cl-Phenyl	0.81 ± 0.16		
50	NH	4-Cl	3,5-diMe-4-Cl-Phenyl	0.16 ± 0.04		
51	NH	4-Cl	1-Naphthyl	0.70 ± 0.24		
52	NH	6-Cl	3-Me-4-Cl-Phenyl	0.19 ± 0.02	>15	1.4
53	NH	6-Cl	3,5-diMe-4-Cl-Phenyl	0.055 ± 0.018	>15	0.87
54	NH	6-Cl	1-Naphthyl	0.075 ± 0.025	6.8	0.96
55	NH	6-Cl	1-(5,6,7,8-tetrahydronaphthyl)	0.066 ± 0.028		
56	NMe	H	3,5-diMe-4-Cl-Phenyl	0.18 ± 0.01	>15	7.4
57	NMe	H	1-Naphthyl	0.26 ± 0.04	>15	>15
58	NMe	6-Cl	3,5-diMe-4-Cl-Phenyl	0.14 ± 0.01		

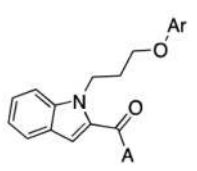
Comp.	A	R	Ar	K _i (μM)		
				Mcl-1 ^a	Bcl-xL ^b	Bcl-2 ^b
59	NBn	H	1-Naphthyl	0.29 ± 0.17	>15	>15
60	S	H	3,5-diMe-4-Cl-Phenyl	0.32 ± 0.01	>15	5.3
23	S	H	1-Naphthyl	0.37 ± 0.07	15	9.7
61	S	4-Cl	3,5-diMe-4-Cl-Phenyl	1.3 ± 0.52		
62	S	4-Cl	1-Naphthyl	1.6 ± 0.41		
63	S	6-Cl	3,5-diMe-4-Cl-Phenyl	0.25 ± 0.04	4.1	0.80
64	S	6-Cl	1-Naphthyl	0.12 ± 0.03	6.8	0.96
65	S	7-Cl	3,5-diMe-4-Cl-Phenyl	0.75 ± 0.24		
66	S	7-Cl	1-Naphthyl	0.72 ± 0.15		
67	O	H	3,5-diMe-4-Cl-Phenyl	3.0 ± 0.10		
26	O	H	1-Naphthyl	1.0 ± 0.44	>15	4.3
68	O	5-Cl	1-Naphthyl	2.5 ± 1.1		

^aK_i values are measured in triplicate

^bK_i values are measured in duplicate

Table 4

SAR of 2-carboxylate analogs on 1-substituted indoles



Comp.	A	Ar	Mcl-1 K_i (μM) [*]
69	OH	3-Me-4-Cl-Phenyl	1.2 \pm 0.43
70	OH	3,5-diMe-4-Cl-Phenyl	0.41 \pm 0.07
71	OH	1-Naphthyl	0.47 \pm 0.08
72	NH ₂	1-Naphthyl	>500

* All K_i values are measured in triplicate

Table 5

X-ray data collection and refinement statistics. Values in parenthesis represent the highest resolution shell

Ligand	53	60	16mer peptide ^a
PDB ID code	4HW2	4HW3	4HW4
No. chains	6	12	2
Protein construct	Mcl-1 Δ5	Mcl-1 Δ5	Mcl-1 WT
Data collection			
Space group	P2 ₁ 2 ₁ 2	P2 ₁	P2 ₁
Cell dimensions			
a, b, c (Å)	121.99, 134.32, 62.04	139.44, 58.76, 140.67	50.07, 48.35, 68.18
α, β, γ (°)	90.00, 90.00, 90.00	90.00, 90.71, 90.00	90.00, 93.83, 90.00
Resolution (Å)	50.00-2.80 (2.85-2.80)	50.00-2.40 (2.44-2.40)	50.00-1.53 (1.56-1.53)
R _{sym}	5.7(29.7)	5.3(29.9)	4.7 (40.8)
R _{merge}	4.5 (41.1)	4.5 (36.4)	4.2 (31.3)
I / σI	5.7 (1.9)	12.5 (4.9)	25.0 (2.5)
Completeness (%)	97.7 (95.0)	98.2 (96.3)	100 (100)
Redundancy	4.1 (3.4)	3.5 (2.7)	4.1 (3.4)
Structure Refinement			
No. reflections	25097	88346	49292
R _{work} / R _{free}	21.69 / 24.52	21.51 / 26.28	13.74 / 18.40
No. atoms			
Protein	7181	14259	4823 ^b
Ligand	190	300	520
Water	-	252	387
Ramachandran (%) ^c			
Preferred regions	90.1	89.9	94.5
Allowed regions	7.4	8.4	5.1
Generously allowed	1.5	1.2	0.3
Disallowed region	1.0	0.6	0.0
RMS deviations			
Bond lengths (Å)	0.026	0.010	0.008
Bond angles (°)	1.993	1.411	1.005

^a16mer Mcl-1 BH3-peptide: Ac-ALETLLRRVGDGVQRNH-NH₂^bIncluding hydrogen atoms^cBackbone conformation was analyzed with PROCHECK⁵²